




Chair of Materials Science and Testing of Polymers

Master's Thesis



Batch variations of post-consumer  
recyclates and their influence on material  
properties

Linda Marlen Schatz, BSc

September 2023



**EIDESSTATTLICHE ERKLÄRUNG**

Ich erkläre an Eides statt, dass ich diese Arbeit selbständig verfasst, andere als die angegebenen Quellen und Hilfsmittel nicht benutzt, und mich auch sonst keiner unerlaubten Hilfsmittel bedient habe.

Ich erkläre, dass ich die Richtlinien des Senats der Montanuniversität Leoben zu "Gute wissenschaftliche Praxis" gelesen, verstanden und befolgt habe.

Weiters erkläre ich, dass die elektronische und gedruckte Version der eingereichten wissenschaftlichen Abschlussarbeit formal und inhaltlich identisch sind.

Datum 30.08.2023

---

Unterschrift Verfasser/in  
Linda Marlen Schatz

---

## ACKNOWLEDGEMENTS

I would like to thank Prof. Dipl.-Ing. Dr. mont. Gerald Pinter as head of the Chair for Materials Science and Testing of Polymers at Montanuniversitaet Leoben, for giving me the opportunity to write my master thesis at his departement. I am grateful for the use of testing equipment in every laboratory and for his support concerning interpretation of results. His experience was leading the way for a successful completion of this thesis.

On behalf of the Polymer Competence Center Leoben GmbH special thanks goes to Dipl.-Ing. Jessica Hinczica for supervising this thesis, her patience and support during the whole process. With her specific experience in that field I was able to master all challenges I faced throughout the extensive material testing, evaluations and summary of the results. She pathed my way as student researcher when she asked me four years ago to join the pipe group. Working with her, was always a pleasure! At this point I would also like to thank her for our long-lasting friendship over all those years - you have definitely enriched my time at university since day one.

I would also like to offer my sincere thanks to Dipl.-Ing. Dr. mont. Mario Messiha (Polymer Competence Center Leoben GmbH) for making this thesis possible in course of the Comet project, his professional support and open ear no matter the task or daytime.

This master thesis was written in the course of the COMET-project „Processing and lifetime performance of virgin pipe grades blended with recyclates“ (Project-No.: VII-3.08) at the Polymer Competence Center Leoben GmbH (PCCL, Austria) within the framework of the COMET-program of the Federal Ministry for Climate Action, Environment, Energy, Mobility, Innovation and Technology and the Federal Ministry for Digital and Economic Affairs with contributions by Montanuniversitaet Leoben, Technical University Wien and DYKA, Fränkische Rohrwerke Gebr. Kirchner GmbH & Co. KG, Pipelife International GmbH, Polypipe Ltd., Rehau AG & Co. KG, European Plastic Pipe and Fittings Association (TEPPFA), Vynova Group, Staatliche Versuchsanstalt – TGM Kunststoff- und Umwelttechnik and Wavin T&I. The Polymer Competence Center Leoben GmbH is funded by the Austrian Government and the State Governments of Styria, Lower Austria and Upper Austria.

My gratitude would be incomplete if I did not mention all friends and companions of the past years. Thanks to all of you who have endured and encouraged me even in tense situations and helped me to keep a cool head by doing all kinds of leisure activities. Lifelong friendships have been built on the road we walked together – Leoben connects.

Last but not least, I am deeply grateful to my family. Thank you, Dad, for awakening my interest in the field of engineering as a child. A special thanks goes to my beloved sister for her open ear all those years and her understanding when I wasn't around - thank you, Lisa. Finally, from the bottom of my heart, I would like to thank my mother for her undeniable moral (and financial) support throughout my entire time at university. Without her it would not be possible to write these lines at all. Mom, this thesis is dedicated to you!

---

## ABSTRACT

The trend to use recyclates as a substitute or supplement for virgin material has become increasingly important in recent years. So far, there are little to no regulations for the quality of a recyclate and no parameters that are required to be fulfilled. The quality of a recyclate depends on the composition of waste and sorting accuracy, which corresponds to the purity of the recyclate. For manufacturers, consistent recyclate quality is of high importance to ensure consistent production processes and required properties of the final products over time.

In Europe, most of the recycled material is processed into new products in the construction industry (PlasticsEurope 2020). Recyclates and blends of recyclates with virgin material are already applied for various parts in the plastic pipe industry (Kunststoffrohrverband e.V. - Fachverband der Kunststoffrohr-Industrie 2022). Currently available recycled polypropylene (PP) types do not fulfill the requirements for long service lifetime due to their lower quality. However, also a small amount of recycled material added to virgin PP grades can already lead to a reduction in service lifetime (Utracki and Wilkie 2014).

For this purpose, a broad variation of properties of a PP post-consumer recyclate (PCR) were investigated over time. Ten batches of a PCR, available on the European market, were ordered from one supplier over a 15 - month period. Thermal, mechanical, rheological and thermomechanical properties were characterized by means of various standard test methods. Since recyclates are used in long-term applications, the lifetime under cyclic load was characterized by means of a cyclic Cracked Round Bar (CRB) test according to (ISO 18489). Additionally, fracture surfaces were examined by light microscopy and Scanning Electron Microscopy (SEM) to evaluate variations in failure mechanisms. Another focus was on the application of (ONR CEN/TS 14541-2), a standard for recommendations on the properties of thermoplastic recyclates for pipes and fittings. It was investigated whether already existing standards provide valid guidelines for the processing of recycled materials in the pipe sector.

High variations were observed in various properties of PP recyclates, especially for results of thermogravimetric analysis (TGA), cyclic cracked round bar (CRB) test and melt flow

rate (MFR). The obtained results show that MFR of the ten batches varies between 6 g/10 min and 12 g/10 min and the amount of inorganic ingredients varies strongly. Six batches have a comparable amount of inorganic components of about 10 %, while one batch nearly has three times the proportion inorganic ingredients. For batches with a high amount of inorganic ingredients notch sensitivity increases. In the conducted CRB tests, all batches showed lower crack resistance under cyclic loading compared to a conventional virgin extrusion grade. Especially, the scattering of results is significantly higher. Differences in MFR and amount of inorganic ingredients are also visible in results of the CRB test. Batches with low MFR lead to a better performance, while a high amount of inorganic ingredients reduces resistance against cyclic load. In addition, it was investigated whether batch variations in the CRB test can be compensated by blending batches with virgin material. It was found, that an addition of 25 % recyclate drastically reduces the resistance against cyclic load of a specific virgin material. However, the results show that mixing virgin material with 25% recycled material cannot compensate for the batch variations of the recycled material.

The CRB test has proven to be a suitable method to rank recyclates in terms of lifetime relevant properties but regulations regarding standard (ONR CEN/TS 14541-2) should be adapted. For other common standard test methods, the allowable property intervals should be reduced to guarantee good quality and sufficient material properties during processing and subsequent product application.

## KURZFASSUNG

Die Herstellung von Produkten aus Rezyklaten anstelle von Neuware hat in den letzten Jahren zunehmend an Bedeutung gewonnen. Bislang gibt es wenig bis keine Vorschriften über die Qualität eines Recyclats und keine Grenzwerte, die erfüllt werden müssen. Die Qualität eines Rezyklats hängt von der Zusammensetzung des Abfalls und der Sortierqualität ab, die der Reinheit des Rezyklats entspricht. Für die Hersteller ist eine gleichbleibende Rezyklatqualität von großer Wichtigkeit, um konstante Herstellungsprozesse und hinreichende Eigenschaften der Endprodukte im Laufe der Zeit sicherzustellen.

In Europa finden Rezyklate größtenteils in der Bauindustrie ihren Weg zurück als neue Produkte (PlasticsEurope 2020). Rezyklate und Mischungen von Rezyklaten mit Neuware werden bereits für verschiedene Anwendungen in der Kunststoffrohrindustrie eingesetzt (Kunststoffrohrverband e.V. - Fachverband der Kunststoffrohr-Industrie 2022). Die derzeit verfügbaren recycelten Polypropylen (PP)-Typen genügen aufgrund ihrer geringen Qualität aber nicht den Anforderungen an eine ausreichend lange Lebensdauer. Wird nur ein geringer Anteil an Rezyklat in neue PP-Typen eingebracht, kann dies schon zu einer Verkürzung der Lebensdauer führen (Utracki and Wilkie 2014).

Zu diesem Zweck ist die Veränderung der Eigenschaften eines Post-Consumer-Rezyklats (PCR) im Laufe der Zeit untersucht worden. Zehn Chargen eines auf dem europäischen Markt erhältlichen PCR wurden über einen Zeitraum von 16 Monaten bei einem Lieferanten bestellt. Die thermischen, mechanischen, rheologischen und thermomechanischen Eigenschaften wurden mit Hilfe verschiedener Standardprüfverfahren charakterisiert. Da Rezyklate auch in Langzeitanwendungen eingesetzt werden, ist die Lebensdauer unter zyklischer Belastung mit dem zyklischen Cracked Round Bar (CRB)-Test nach (ISO 18489) charakterisiert worden. Zusätzlich sind Bruchflächen lichtmikroskopisch und mit dem Rasterelektronenmikroskop (REM) untersucht worden, um Unterschiede im Versagensmechanismus zu bewerten. Ein weiterer Schwerpunkt war die Anwendung der (ONR CEN/TS 14541-2), einer Norm für Empfehlungen zu Eigenschaften von thermoplastischen Rezyklaten für Rohre und

Formstücke. Es wurde überprüft, ob diese bisher gültigen Standards brauchbare Anhaltspunkte in Bezug auf die Verarbeitung von Rezyklaten im Rohrbereich liefern.

Es wurden große Schwankungen bei unterschiedlichen Materialeigenschaften von PP-Rezyklaten festgestellt, vor allem für die Ergebnisse aus der thermogravimetrischen Analyse, dem zyklischen Cracked Round Bar (CRB)-Test und der Schmelzfließrate (MFR). Die Ergebnisse zeigen, dass die MFR Werte der zehn Batches zwischen 6 g/10 min und 12 g/10 min schwanken und auch der Anteil der anorganischen Bestandteile stark variiert. Sechs der zehn Batches haben einen vergleichbaren Anteil an anorganischen Inhaltsstoffen von etwa 10 %, während ein Batch beinahe den dreifachen Wert an anorganischen Bestandteilen aufweist. Bei hochgefüllten Batches nimmt die Kerbempfindlichkeit zu. Im CRB-Test zeigen alle Batches eine kürzere Lebensdauer unter zyklischer Belastung im Vergleich zu einer konventionellen, fabrikneuen Extrusionstypen. Insbesondere die Streuung der Ergebnisse ist deutlich höher. Unterschiede des MFR und der Menge der anorganischen Bestandteile sind auch in den Ergebnissen des CRB-Tests sichtbar. Batches mit einem niedrigen MFR führen zu einer längeren Lebensdauer, während ein hoher Anteil von anorganischen Bestandteilen den Widerstand gegen zyklische Belastung reduziert. Darüber hinaus wurde untersucht, ob die Batchvariationen im CRB-Test durch die Mischung der Batches mit Neuware kompensiert werden können. Die Ergebnisse zeigen jedoch, dass das Mischen von Neuware mit 25 % Rezyklat die Chargenschwankungen des Rezyklats nicht kompensieren kann. Die Zugabe von 25 % Rezyklat zu einer bestimmten Neuware verringerte den Widerstand gegen Risswachstum drastisch.

Der CRB-Test hat sich als geeignetes Verfahren erwiesen, um Rezyklate hinsichtlich lebensdauerrelevanter Eigenschaften einzustufen, doch müssen die Normvorschriften angepasst werden. Bei anderen gängigen Standardprüfverfahren sollten die zulässigen Eigenschaftsintervalle verringert werden, um gut Qualität und ausreichende Materialeigenschaften bei der Verarbeitung und späteren Produktanwendung zu gewährleisten.



## TABLE OF CONTENT

<b>SYMBOLS AND ABBREVIATIONS .....</b>	<b>1</b>
<b>TABLE OF FIGURES.....</b>	<b>4</b>
<b>1 INTRODUCTION AND OBJECTIVES.....</b>	<b>7</b>
<b>2 BACKGROUND .....</b>	<b>9</b>
2.1 Polypropylene.....	9
2.1.1 Chemical structure, related properties and applications of polypropylene .....	9
2.1.2 Cross contamination of polypropylene and polyethylene .....	13
2.2 Recycling.....	14
2.2.1 Recycling of plastic waste.....	15
2.2.2 Standards and regulations for recyclates.....	18
2.2.3 Circular economy action plan.....	22
2.3 Fillers and their and influence on material properties.....	23
2.3.1 Talc.....	24
2.3.2 Calcium carbonate.....	26
<b>3 EXPERIMENTAL.....</b>	<b>28</b>
3.1 Material selection.....	28
3.2 Material characterization and test methods.....	29
3.2.1 Density.....	30
3.2.2 Melt flow rate.....	30
3.2.3 Rheometric experiments .....	31
3.2.4 Thermal analysis .....	32
3.2.5 Thermogravimetric analysis .....	34
3.2.6 Dynamic mechanic analysis .....	35
3.2.7 Fourier Transform Infrared Spectroscopy .....	35

---

3.2.8	Tensile test.....	37
3.2.9	Charpy impact test .....	38
3.2.10	Lifetime under cyclic load via CRB test.....	39
<b>4</b>	<b>RESULTS AND DISCUSSION .....</b>	<b>41</b>
4.1	Density.....	41
4.2	Rheological analysis.....	42
4.3	Thermal analysis .....	44
4.4	Thermogravimetric analysis .....	46
4.5	Dynamic mechanic analysis .....	47
4.6	Fourier Transform Infrared Spectroscopy .....	48
4.7	Tensile test.....	50
4.8	Charpy impact test .....	52
4.9	Lifetime under cyclic load via CRB test.....	54
<b>5</b>	<b>SUMMERY AND CONCLUSION .....</b>	<b>61</b>
<b>6</b>	<b>PUBLICATION BIBLIOGRAPHY .....</b>	<b>64</b>

**SYMBOLS AND ABBREVIATIONS**

$a_{cN}$	Charpy notched impact strength
$a_{cU}$	Charpy unnotched impact strength
aPP	Atactic polypropylene
B	Batch
C	Carbon
$CaCO_3$	Calcium Carbonate (chalk)
CRB	Cracked round bar
D	Degree of crystallinity
DMA	Dynamic Mechanic Analysis
DSC	Differential Scanning Calorimetry
E	Young's modulus
$E^*$	Complex Young's modulus
$E'$	Storage modulus DMA
$E''$	Loss modulus DMA
$\varepsilon_b$	Elongation at break
EU	European Union
f	Frequency
FTIR	Fourier-transform infrared spectroscopy
$G'$	Storage modulus
$G''$	Loss modulus
H	Hydrogen
$\Delta H_m$	Enthalpy
iPP	Isotactic polypropylene

---

$k_z$	Notch sensitivity
MFR	Melt Flow Rate
MVR	Melt Volume Rate
$M_w$	Molecular weight
$N_f$	Number of cycles until failure
NIR	Near Infrared Spectroscopy
O	Oxygen
OOT	Oxidation Onset Temperature
PE	Polyethylene
PET	Polyethylene terephthalate
POM	Polyoxymethylene
PP	Polypropylene
PP-H	Polypropylene homopolymer
PVC	Polyvinylchloride
R	Radius
SEM	Scanning Electron Microscopy
sPP	Syndiotactic polypropylene
$\sigma_Y$	Yield stress
$\tan \delta$	Loss factor
$T_c$	Decomposition temperature
TDS	Technical data sheet
$T_g$	Glass transition temperature
TGA	Thermogravimetric Analysis
$T_m$	Melting temperature

$T_N$  Secondary softening temperature

vPP Virgin polypropylene

**TABLE OF FIGURES**

Figure 1:	World plastics demand in 2021 (PlasticsEurope 2022).....	7
Figure 2:	Semi-crystalline structure with crystalline and amorphous regions connected via tie molecules (Domininghaus et al. 2012). ....	10
Figure 3:	Tacticity of PP a) iPP, b) sPP and c) aPP (Domininghaus et al. 2012). ....	11
Figure 4:	Structure of random (PP-R) and block (PP-B) copolymerized PP molecules. Letters P and E represent PP and PE monomer units, respectively (Tripathi 2002).....	12
Figure 5:	Difference in structure, PE (left) and PP (right) (Guerrilla Agency 2022).....	14
Figure 6:	Annual production of plastics worldwide from 1950 to 2021 based on (Statista 2023).....	15
Figure 7:	Information on properties of recycled PP from evaluated technical data sheets (Hans-Josef Endres and Madina Shamsuyeva 2020).....	20
Figure 8:	Failure cycle numbers $N_f$ as a function of the applied stress range $\Delta\sigma$ , schematic representation of the pass/fail criteria for the cracked round bar test (ONR CEN/TS 14541-2). ....	22
Figure 9:	Results of cracked round bar (CRB) test of talc filled (triangle) and non-talc filled (circle) PP, tested at 80 °C in quasi-brittle failure mode (Florian J. Arbeiter et al. 2016).....	26
Figure 10:	Batches under investigation, time interval from August, 2021 to November, 2022.....	28
Figure 11:	Material blend M1 and M2.....	28
Figure 12:	Geometry of a plate-plate rheometer (Grellmann 2011). ....	31
Figure 13:	Enthalpy change $\Delta H_m$ for semi-crystalline thermoplastics at constant heating rate above glass transition region, determination of crystallite melting temperature $T_m$ (Ehrenstein et al. 2003).....	32

Figure 14: Schematic DSC curve showing applied method for separate calculation of enthalpy $\Delta H_m, PE$ , and $\Delta H_m, PP$ .....	33
Figure 15: Typical TGA curve with single step mass loss.....	34
Figure 16: FTIR spectra of virgin polypropylene (PP). .....	36
Figure 17: a) Spectrum of talc (University of Tartu 2023a) , b) Spectrum of chalk (University of Tartu 2023b). .....	37
Figure 18: Makro positioning on multipurpose specimen, tensile test setup. ....	38
Figure 19: Different regions of SEM images taken.....	40
Figure 20: Density measured by balance (left), melt density (right).....	41
Figure 21: Left: Melt flow rate (MFR), right: Melt volume rate (MVR), both measured at 230 °C with 2.16 kg.....	42
Figure 22: Plate-plate rheometer; T=230 °C, left: shear viscosity $\eta$ as a function of shear rate $\dot{\gamma}$ , right: shear viscosity $\eta$ at a frequency of $\omega = 0,001$ rad/s.....	43
Figure 23: Storage modulus $G'$ and loss modulus $G''$ over shear rate $\dot{\gamma}$ , determination of cross over point. ....	43
Figure 24: Heat flow $Q_n$ over temperature $T$ of the second heating curves. ....	45
Figure 25: Left: melting temperature $T_m$ , right: crystallinity $D$ . ....	45
Figure 26: Left: TGA curves (residual weight over temperature), right: residual weight in % of each batch at 750 °C.....	46
Figure 27: Storage modulus $E'$ over temperature $T$ for B1 – 10.....	47
Figure 28: Loss modulus $E''$ for B1-10, pronounced peak at - 50°C (top left), small peak at - 50 °C (top right), no peak at -50 °C (bottom center). ....	48
Figure 29: Representative FTIR spectra for B1-B10.....	49
Figure 30: Comparison of B1, B9 and B2 considering talc band (blue framed), respectively $\text{CaCO}_3$ band (green framed). ....	50
Figure 31: Representative stress-strain ( $\sigma$ - $\epsilon$ ) graphs for B1-B10.....	51

---

Figure 32: Blowholes of B3, B4, B8 and B9.....	51
Figure 33: Young's modulus $E$ (top left), yield stress $\sigma_Y$ (top right), strain at break $\varepsilon_B$ (bottom center) for B1-B10.....	52
Figure 34: Charpy impact test, B2 tested specimens, left: unnotched, right: notched. ..	52
Figure 35: Unnotched impact strength $\alpha_{CU}$ (top left), notched impact strength $\alpha_{CN}$ (top right), notch sensitivity $k_z$ (bottom center) for B1-B10.....	53
Figure 36: Failure cycle numbers $N_f$ as a function of the applied stress range $\Delta\sigma_0$ for B1-B10 (ISO 18489).....	55
Figure 37: Failure cycle numbers $N_f$ as a function of the applied stress range $\Delta\sigma_0$ , comparison best (B2, B10) and worst (B1, B5) performance, B7 with steeper slope. ....	56
Figure 38: Failure cycle numbers $N_f$ as a function of the applied stress range $\Delta\sigma_0$ , different possibilities of regression for B5. ....	57
Figure 39: SEM analysis for B1 (left) and B5 (right).....	58
Figure 40: Failure cycle numbers $N_f$ as a function of the applied stress range $\Delta\sigma_0$ , vPP and blends M1 and M2.....	59



## 1 INTRODUCTION AND OBJECTIVES

Sustainability, recycling and the circular economy are topics that play a central role in society nowadays. As a result, the focus in recent years has been strongly shifted on these topics, not only in Europe but worldwide. In 2021, nearly 391 million tons of polymers were produced globally and for the first time post-consumer recycled polymers are included in the production statistics with a share of 8.3 % (see Figure 1).

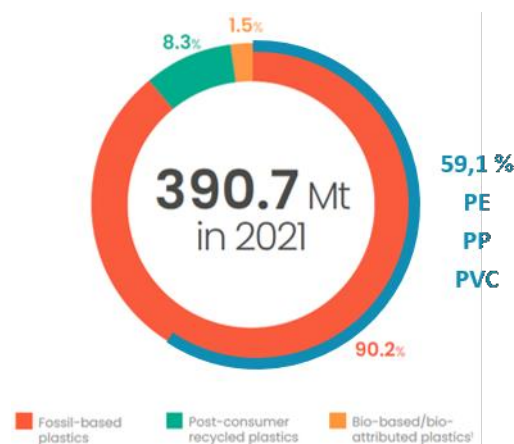


Figure 1: World plastics demand in 2021 (PlasticsEurope 2022).

Post-consumer recycle (PCR) is a term used to describe material manufactured from plastic products that have fulfilled their intended purpose or can no longer be used. Due to the large number of polymers produced, the amount of waste generated also increases annually. Polypropylene (PP) is the most commonly used polymer, accounting for around 20 % of the total and is mainly utilized for short-life packaging applications. However, due to PP's versatile properties, it is also used for durable products in building and construction industry or applications where long service lifetime is required (Kunststoffrohrverband e.V. - Fachverband der Kunststoffrohr-Industrie 2023).

In 2020, around 30 million tons of post-consumer plastic waste was collected in the European Union (EU). Out of this, about one-third was sent to a recycler. Although the trend is increasing, only 15 % of the total post-consumer waste collected was returned to the European economy as recycled plastics in the following year. With 43 %, most products based on recyclates are destined for construction sector. In this application, the material is expected to fulfill a service lifetime of up to 100 years. Due to this, the long-term performance of recyclates is of high interest. Pure recyclates are used in pipe industry for

cable trays, stormwater management and drainage. In wastewater applications, on the other hand, the recyclate is mixed with virgin material to improve part properties (Kunststoffrohrverband e.V. - Fachverband der Kunststoffrohr-Industrie 2023; PlasticsEurope 2020).

Material development for long-term applications is continuously changing the material formulation to improve specific properties or to fit given requirements. Focus now is to bring more recycled material into circular economy including long-term applications. Thus, it becomes increasingly difficult to achieve this without losing important properties such as mechanical and thermal properties.

Plastic recyclates are still limited in their applications because of their significantly lower and inconsistent quality compared to virgin materials. In addition to contamination by other materials or other polymers, mixing of different grades of the same polymer hinders the utilization of recyclates in demanding applications because of property change. Best case, quality and properties of one specific material is always constant and reproducible. Nevertheless, quality of PCR varies depending on origin, feedstock, collection, sorting, treatment and processing of waste (Ammar O et al. 2017a; Ragaert et al. 2017; Geier et al. 2023a).

Presently, there are few standards for quality control or consistency of recyclates, but mostly specifications are just based on agreements between suppliers and converters. Therefore, the manufacturer has to analyze each batch in advance through a quality control process to ensure that the materials meet required specifications and also adapt processing procedures for the new batch. This requires a lot of time and additional resources, as well as higher production costs.

In this thesis, the change of a certain recyclate over a period of time in terms of mechanical, thermal and rheological properties was investigated. Furthermore, the amount of inorganic ingredients and the lifetime under cyclic loading were analyzed. The aim is to determine whether batch variations are present and, if so, how strongly they affect material properties in qualitative and quantitative way.

## 2 BACKGROUND

This chapter provides an overview of the material polypropylene (PP), its properties and field of applications. As one of the most polarizing and challenging topics worldwide at present time, recycling, the recycling process and already existing standards and regulations for recyclates are highlighted as well. Concluding the chapter, fillers are introduced, where talc and chalk ( $\text{CaCO}_3$ ) are examined more in detail.

### 2.1 Polypropylene

In the following, chemical structure and properties of PP are described and their relationship to morphology and thermomechanical properties is explained more in detail. Additionally, processing and application options for PP as well as polyethylene (PE) contaminated PP and PP blends will be discussed.

#### 2.1.1 Chemical structure, related properties and applications of polypropylene

Polypropylene is the most widely used plastic in the world after PE. Its main areas of application are the packaging, fiber and increasingly also the automotive sector. The material is characterized by its low density, high melting point, good processability and numerous possibilities for adjusting mechanical properties. In addition, it excels with a low tendency to stress cracking and food-safe properties (Domininghaus et al. 2012).

It is a semi-crystalline material that exhibits amorphous (non-oriented) zones between the crystalline (orientated) areas with a melting temperature ( $T_m$ ) between 160 °C-165 °C (Ehrenstein et al. 2012). Tie molecules connect crystalline zones with amorphous zones. Individual regions and tie molecules of the semi-crystalline structure of PP are shown in Figure 2. A higher number of tie molecules and amorphous entanglements leads to an increasing toughness and elongation at break (Lustiger 1986; Lustiger and Ishikawa 1991; Pinter 1999; Fiedler et al. 1987).

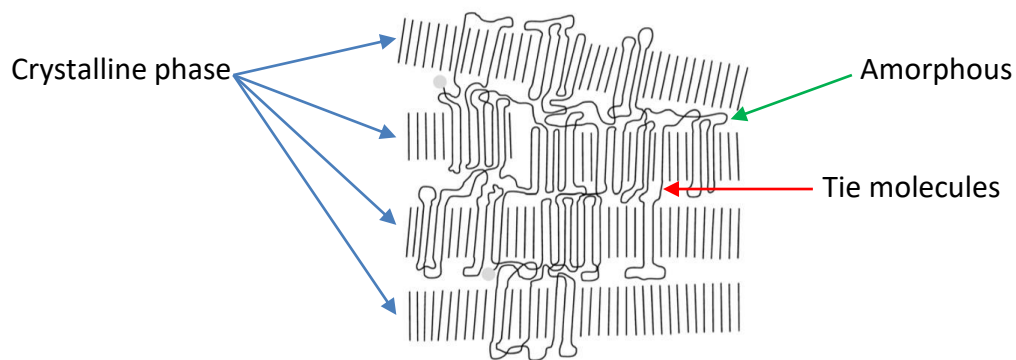


Figure 2: Semi-crystalline structure with crystalline and amorphous regions connected via tie molecules (Domininghaus et al. 2012).

The key to understanding the mechanical properties of plastics at different temperatures is knowledge of the processes in the transition region between the defined states, that is glass transition and melting for semi-crystalline polyolefines. Below glass transition temperature ( $T_g$ ) is the energy-elastic (hard-elastic) state, which is usually characterized by high brittleness. The energy-elastic range and the  $T_g$  are followed by the entropy-elastic (soft-elastic or ductile-elastic) range when heated further, which is the area of application for semi-crystalline polyolefines. For a PP-homopolymer (PP-H)  $T_g$  is reached at  $\sim 0^\circ\text{C}$  (Domininghaus et al. 2012). For some polymers a so called  $\beta$  – transition ( $T_n$ , secondary transition), a softening of -CH<sub>2</sub>- chain segments can take place. Materials with a higher degree of branching show  $T_n$  at a temperature way before  $T_g$ . At  $T_n$  the beginning of rearrangements of molecular segments or of side groups may take place (Ehrenstein 2011).

The bridge between chemical structure, processing, thermo-mechanical history and product properties is morphology. Properties of PP are strongly dependent on molecular structure as well as the production of the polymer by choice of catalysts, polymerization and compounding. Typical catalyst systems for PP are Ziegler-Natta catalysts or modern metallocene systems, i.e. combination of titanium trichloride with tributyl aluminum. Significant PP-homopolymer (PP-H) properties change with the stereospecific catalyst systems applied. They are called stereospecific due to their capability to control the positions of the methyl-groups in each propylene unit of the PP chain. This stereoregulation is known as tacticity, whereby a distinction is made between three forms (Tripathi 2002). Methyl groups (CH<sub>3</sub>) of the macromolecule can be arranged differently relative to the backbone of the polymer chain (configuration) with the same constitution. If the

arrangement is regular, it is called isotactic (iPP). If the methyl groups are arranged in alternating order, it is referred to as syndiotactic PP (sPP) and with irregular arrangement as atactic PP (aPP). The crystallization ability of PP and its degree of crystallinity is essentially determined by the tacticity of the molecular chain. Isotactic PP has a high degree of order and thus a high crystallinity. The three different forms are schematically shown in Figure 3. Tacticity of PP can be varied to a large extent. Components made of iPP, which are produced in typical industrially used processes, have degrees of crystallinity between 30 - 60 %. When sPP is used, degree of crystallinity is lower. Atactic PP is mostly amorphous and does not crystallize (Domininghaus et al. 2012).

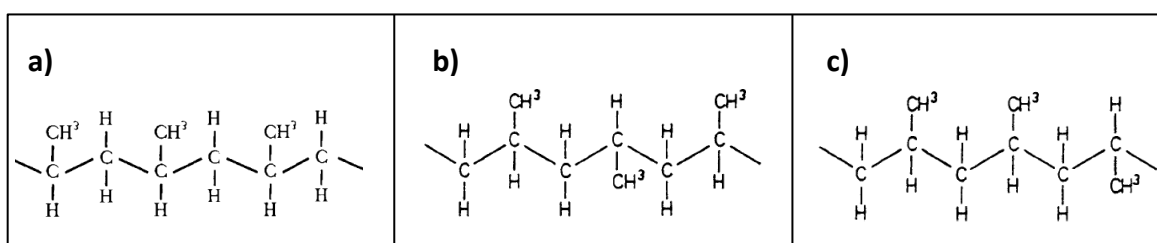


Figure 3: Tacticity of PP a) iPP, b) sPP and c) aPP (Domininghaus et al. 2012).

With a high stiffness, large tensile strength and hardness, semi-crystalline iPP represents the most essential form from a technical point of view. Morphologically, the structure of PP is very complex. In the crystalline region, it can exist in various modifications, which differ in the formation of the crystal lattice and the arrangement of the molecular chains. Depending on the processing conditions, iPP can have  $\alpha$ ,  $\beta$ ,  $\gamma$  or even mesomorphic crystal modifications. The  $\alpha$ -modification is the most prevalent in iPP. The  $\beta$ -modification has a lower degree of order, which is reflected in a higher crystallization rate and a lower  $T_m$ . During isothermal crystallization from the melt of sPP, radially arranged lamellae form. The formation of large spherulites in sPP remains an exception. Atactic PP, on the other hand, is characterized by a random steric orientation of the methyl groups on the carbon atoms along the molecular chain. Due to its amorphous nature, aPP can easily be dissolved in a variety of solvents such as aliphatic and aromatic hydrocarbons, even at moderate temperatures, compared to iPP. In the past, aPP was a by-product of iPP polymerization (Domininghaus et al. 2012).

Due to modifications of the molecular structure to improve the material properties, different types of PP are offered. Typically, ethylene units or higher molecular weight

alkenes (e.g., butene) or thermoplastic elastomers are used as comonomers for PP. Due to the varying copolymerization processes, a distinction is made between three categories, the homopolymer (PP-H) which only consists out of PP, the random copolymer (PP-R) and the block copolymer (PP-B) (Stafford 2001). In Figure 4 structures of random PP copolymer (PP-R) and block copolymer is depicted. While most commercially available isotactic PP-H have higher stiffness and thermal stability compared to their copolymers, long-term properties, such as lifetime under cyclic load, are limited, especially at sub-zero temperatures. This, on the other hand, is not a problem when thinking of very thin sheets or film applications such as in the packaging sector. However, pipe applications with thicker walls usually suffer from embrittlement, which has led to the development of copolymerized forms of PP in recent decades. With copolymerization flexibility and toughness of the material at low temperatures are improved by lowering the  $T_g$ .

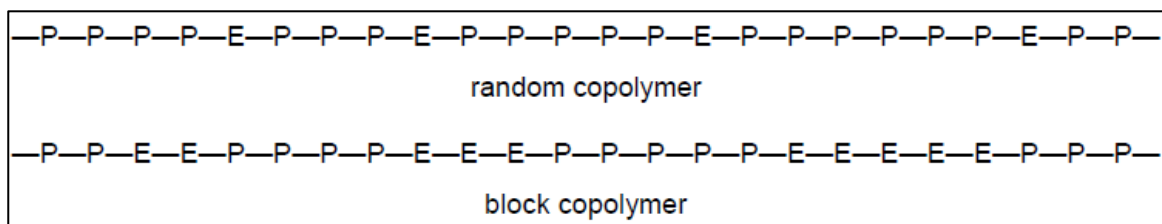


Figure 4: Structure of random (PP-R) and block (PP-B) copolymerized PP molecules. Letters P and E represent PP and PE monomer units, respectively (Tripathi 2002).

Consequently, PP-R is used for small-diameter flexible pipes for hot water distribution because it has lower strength but higher flexibility with similar thermal resistances compared with PP-H. In contrast, PP-B has lower strength but higher fracture toughness at 0 °C. The block segments formed at the molecular level result in a heterophasic microstructure, which is necessary to prevent cracking, making it a suitable material for buried pipes such as drainage or sewerage (Stafford 2001; Dominghaus et al. 2012).

Following the chemical structure, chain length of a polymer and its distribution is one of the most important molecular parameters controlling the mechanical, physical and processing properties of thermoplastics. Mechanical properties, for example, can be tailored by changing the molecular weight ( $M_w$ ). The lower the average  $M_w$  of polymer chains, the smaller the degree of entanglement. Thus, shorter chains slip more easily from one another when they are subjected to mechanical stress resulting in lower toughness, while longer chains increase the ductility and fracture resistance (Touris et al. 2020).

Many properties of PP are determined by its  $M_w$  weight. Higher molecular weight grades are tough and flexible, while lower molecular weight grades are stiff, hard and sensitive to impact. Weight average of iPP is between 200.000 - 600.000 g/mol, where high  $M_w$  result in high melt strength, which is important for the extrusion process. Thermo-mechanical properties depend especially on size and type of crystal structures, which can be influenced by cooling rate and nucleation. Injection molded parts made from PP grades with a narrow molar mass distribution shrink less and almost independently of direction. This results in lower residual stresses and warpage, less white fracture and higher transparency, which speaks for good product quality. (Domininghaus et al. 2012).

Due to its low price and excellent properties, it can be found in an unusually wide range of applications. Packaging sector accounts for 40 % followed by building and construction with 20 % and automotive applications with around 10 % of PP applications (PlasticsEurope 2020). Numerous PP grades are available on the market whose property profiles have been "tailor-made" specifically for the corresponding applications. Property spectrum ranges from robust stiff variants for automotive components to soft flexible fibers for baby diapers.

Regarding injection molding PP is used for of large-volume components, so called "white goods" like washing machines, dishwashers, kitchenware, etc.. Regarding automotive industry it is applied extensively for large components such as bumpers. In addition to injection molding, PP is also processed in large quantities by extrusion. Semi - finished products like pipes, profiles, sheets and wire sheathing are extruded with PP as well as blow molding films for packaging and insulation. For packaging applications, especially films, materials must have high gloss and transparency as well as high strength. For these applications mainly PP is used as it provides those optical properties and furthermore, its tendency to form stress cracks is lower than for PE. (Domininghaus et al. 2012).

### **2.1.2 Cross contamination of polypropylene and polyethylene**

The polyolefins PE and PP are recognized as indispensable materials in this society, but their differentiation (recyclability) turns out to be difficult. Many products are designed as a combination of both materials to gain tailored material properties, such as PP bottles with

PE caps in common household items. Looking more closely at the molecular structures of these polymers, it is obvious that there are only minor differences in their chemical structure. They differ just by one additional methyl group instead of a hydrogen atom for each monomer, depicted in Figure 5.

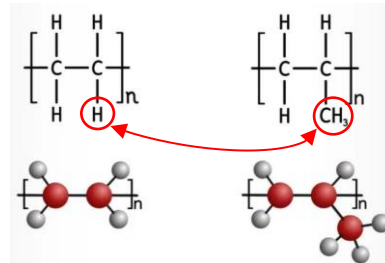


Figure 5: Difference in structure, PE (left) and PP (right) (Guerrilla Agency 2022).

Physical properties of the two materials are also quite similar. A cost-effective separation method of plastic waste is based on the different densities of the materials. But in case of PE and PP this becomes extremely difficult, as both polymers are indistinguishable to the naked eye and even have similar specific gravity. Separation by conventional sink float methods used in plastics recycling industry is possible but with limitations. Near-field infrared (NIR) technologies represent state of the art for further separation between the two polyolefins. In reality, 100 % pure waste separation cannot be assured. Regardless of the specific application areas of PP and PE, the annual production increases year by year which makes the need and desire for sufficient recycling solutions inevitable. Since PE and PP are highly immiscible, a significant influence on the mechanical short-term and long-term properties due to the respective cross-contamination have been found (Messiha et al. 2020).

## 2.2 Recycling

In this section, basic definitions concerning recycling are explained. This chapter also contains a description of the phases a plastic product goes through during its service life and its end of life possibilities. The second part deals with already existing standards and regulations for recyclates. It is discussed, what influence recyclates have on virgin materials, regarding property change and the regulations for the utilization of recyclates in new products is discussed. Finally, aspects of the circular economy action plan of the European Commission are listed.



Before a recycling process can be implemented, waste has to be produced. In the European Union (EU) waste is considered as “any substance or object which the holder discards or intends or is required to discard”. After a part is discarded, the waste management starts operating which involves collection, transport, recovery and disposal of waste, including the supervision of such operations and the after-care of landfills. Another way for plastic waste to end up would be incineration for energy recovery. Nevertheless, the goal is to recycle as much material as possible. Recycling is defined as "any recovery operation by which waste materials are reprocessed into products, materials or substances whether for the original or other purposes" (European Union 2008).

### 2.2.1 Recycling of plastic waste

Plastics are inexpensive, lightweight, durable and easy to shape. A life without plastics would be indispensable for our society. Due to their versatility in everyday life and other advantages, they have largely replaced traditional materials. This is why plastic production has increased rapidly over the last 70 years from 50 million tons to 391 million tons per year (see Figure 6) (Statista 2023).

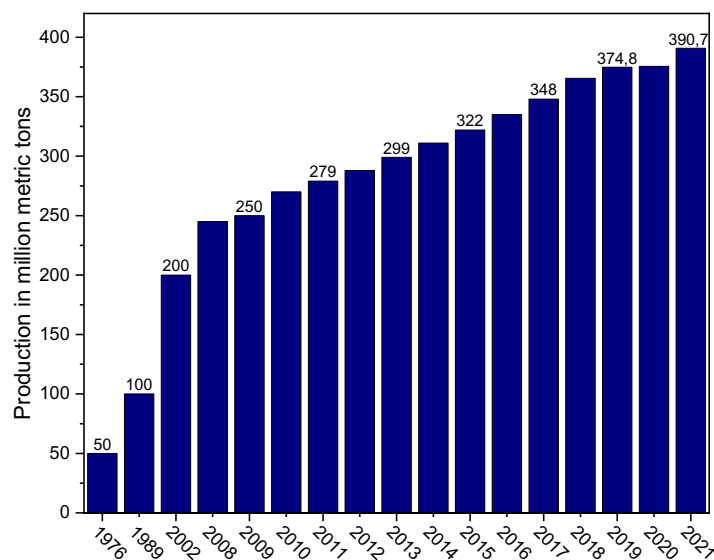


Figure 6: Annual production of plastics worldwide from 1950 to 2021 based on (Statista 2023).

Currently, recyclates are divided into two categories: pre- and post-consumer recyclates. While PCR are made from products that have served their purpose and can no longer be utilized, pre-consumer recyclates are plastic residues generated during industrial processing of virgin plastics.

Pre-consumer waste is usually easier to separate in advance by composition, so sorting is much more commonly used for post-consumer waste than for pre-consumer waste. Same applies for washing, as post-consumer waste is usually more contaminated (Ragaert et al. 2017). Sources of pre-consumer PP are also diverse and include various components from injection molding, extrusion (including films and sheets) and fiber production.

In a circular economy, PCR is an essential component, as it is an important raw material source. Its adoption reduces the amount of waste and can additionally decrease the need for virgin materials (Cornell 2007; Ignatyev et al. 2014). Primary raw material source for PP recyclates is food and non-food packaging. Sources for post-consumer PP are typically drinking bottles, bottle caps, food trays, pans and a variety of containers. This fact is associated with problems in separating food grade and non-food grade PP waste during collection and sorting (Recycled PP - cirplus 2023).

Waste prevention is still the most favorable option. Unfortunately, society works differently and 23 % of collected waste was landfilled in 2020. Another possibility for waste to end up is energy recovery, which, in 2020, accounted for 42 %. Recycling is the most desirable route for a used plastic product after waste prevention (PlasticsEurope 2022). Under "ideal conditions" PP is very easy to recycle. This applies to multiple processing steps, which, if sufficient stabilization available, leads to practically no loss in mechanical properties of the material. Problems arise due to modifications of the polymer and stresses during the application. For example, polymer impurities, other material impurities or poorly separated coatings can lead to defects in recycled material (Domininghaus et al. 2012). Also, the crystallite structure changes, and quality losses are observed in color and odor. In case of insufficient stabilization, too high shear or too high processing temperature, degradation of molecular weight takes place.

Another issue that arises with recycling of post-consumer plastic waste are seasonal effects. Yet, no study was found that explicitly examined pre-sorted waste bales, with regard to seasonal variations and separation by processing methods.

However, seasonal variations in the composition of waste exist, which is one of the reasons for inconsistent quality of the recyclates. This underlines the importance of proper sorting and treatment of waste bales before reprocessing, in order to obtain high quality recyclates with reasonably consistent quality. Reasons for seasonal variations can include changes in waste sources, changes or differences in sorting systems used, or general seasonal variations in the composition of plastic packaging waste. They may result from the fact that certain products are used in smaller or larger quantities at certain times of the year. Examples might be the barbecue season in summer, when packaged barbecue food, lots of sauces in plastic bottles, disposable tableware or ice cream packaging are increasingly used (Geier et al. 2023b)

In this thesis, focus lies on mechanical recycled PCR - PP, as it is the most common option. It refers to the processing of plastic waste by physical means back to plastic products where the chemical structure of the material remains the same (Villanueva Krzyzaniak and Eder 2014). General steps of the mechanical recycling process are as listed below.

- Separating and sorting - based on shape, density, size, color, chemical composition
- Baling - for transportation purposes, if plastic is not processed where it is sorted
- Washing - removal of impurities, often organic
- Grinding - shredding of products into flakes
- Compounding and pelletizing - optional further processing of flakes into pellets, easier to handle than flakes

Before recycled materials are actually reprocessed into new products, a conversion of waste into new raw materials has to take place. For solid plastic waste, this process can include each of the steps, of which each can occur several times or not at all. Separation and sorting are one of the most important steps in the recycling process of post-consumer plastic waste. Without improved sorting of post-consumer waste streams, it is not possible to produce recyclates with suitable processing properties (e.g., MFR values). Sorting by processing method has an enormous positive effect on the MFR value. By reducing the MFR

value of recyclates through improved sorting, a higher percentage of the recyclate can be used for extrusion, blow molding or thermoforming applications. For these processing methods a low MFR is good to achieve high melt strength. Sorting systems that allow sorting by processing methods are needed to obtain recyclates with higher and more important consistent quality (Geier et al. 2023a; Ragaert et al. 2017; Ehrenstein 2011).

Regranules out of PP are suitable for injection molding as well as for a variety of extrusion applications. Similar to virgin materials, recycled PP has valuable material properties, such as high tensile and impact strength, good fatigue resistance and high chemical resistance to most organic solvents, many acids and bases at room temperature. The density of pure PP recyclates (without fillers or reinforcing materials) ranges from 0.90 to 0.92 g/cm<sup>3</sup> and is comparable to virgin PP. To produce high-quality products and meet application-specific requirements or improve the final material performance, recycled PP is usually blended with virgin PP by up to 50 %. However, before blending virgin polymers with non-virgin ones, it is essential to consider the impact of the pre- and post-consumer recyclates on the lifetime-relevant properties of new products. Another way to meet application-specific requirements, material properties of recycled PP can be improved by using additives such as fillers or reinforcing agents, stabilizers or color masterbatches (Recycled PP - cirplus 2023).

Aspects as the influence of polymeric impurities (e.g., amount of virgin PE or other materials in virgin PP, etc.), polymeric additives and inorganic ingredients (e.g. amount of fillers, etc.) and changes in molecular mass and molecular mass distribution due to reprocessing steps during recycling need to be investigated (Messiha et al. 2020).

### **2.2.2 Standards and regulations for recyclates**

Vast quantities of plastic do not make it into the recycling loop, but end up in incineration or even worse in landfills. High-quality plastic recyclates are sometimes not available and in some cases their use is actually more expensive than virgin material. Processing plastic waste into recyclates, that can be reused in products of equal or higher value, is still a challenge plastic industry is facing. The cause is strong variation in quality of recyclates (Fischer 2021).

Nevertheless, interest in high-quality recyclates is growing. However, corresponding suppliers complain about a lack of customers. Key reason is the missing reliable and comprehensive quality standards for recyclates. If there are no specifications to clearly regulate quality of a recyclate, the value for it cannot be quantified and the recyclate cannot be traded. An important requirement for a well-functioning circular economy is therefore a much greater emphasis for broad quality standards for generated recyclates, a consistent design for recycling and a recycling-friendly material and product design to enable their reuse. On a governmental level, regulations and laws are increasingly being enacted that limit single-use plastic products and/or require increased recycling rates, following the example of paper, glass or metal. However, the inexpensive petrochemical feedstock for virgin materials make high-quality and effective plastics recycling difficult.

In the field of plastics recycling, a number of new standards have been developed and published, particularly within the last ten years. In Table 1 some standards regarding recycling are listed. These standards are differentiated according to standards targeting specific plastic products, general aspects such as terminology, sampling, test methods and material-specific standards that exist for most important commodity plastics (Hans-Josef Endres and Madina Shamsuyeva 2020).

Table 1: Overview of important standards in the field of plastics recycling (based on (Hans-Josef Endres and Madina Shamsuyeva 2020)).

	<b>Standard</b>	<b>Title/content</b>
<b>Polymer specific standards</b>	DIN EN 15344	Characterization of polyethylene (PE) recyclates
	DIN EN 15345	Characterization of polypropylene (PP) recyclates
	DIN EN 15346	Characterization of polyvinylchloride (PVC) recyclates
<b>Product specific standards</b>	DIN EN 13430	Requirements for packaging recoverable by material recycling
	DIN EN 13437	Packaging and material recycling- Criteria for recycling methods
<b>Standards for terminology, sampling, test methods</b>	DIN CEN/TS 16010/ DIN SPEC 91010	Sampling procedures for testing plastics waste and recyclates
	ISO 15270	Guidelines for the recovery and recycling of plastics waste
	DIN EN 15343	Plastics recycling traceability and assessment of conformity and recycled content

Another problem for proper use of recyclate is the lack of information a manufacturer gets. According to the journal *Plastverarbeiter* (Hans-Josef Endres and Madina Shamsuyeva 2020) there are recyclates whose technical data sheets (TDS) contain very little information and characteristic values about the material. Moreover, in some cases it is also not stated how values were determined. Ideally, information on various technical properties should be as comprehensive as possible and based on relevant test standards. An evaluation of TDS of several commodity plastics supplied by different companies with regard to quantity and quality of material data was published from *Plastverarbeiter* (Hans-Josef Endres and Madina Shamsuyeva 2020). For PP, 51 TDS from eleven companies have been taken under investigation. Results of the evaluated TDS for relevant material properties of PP are shown in Figure 7. Green marks sufficient and comprehensible values in accordance with the standard, yellow represents values including test parameters. Orange indicates data not in accordance with a standard or visual inspection and red means no information at all (Hans-Josef Endres and Madina Shamsuyeva 2020).

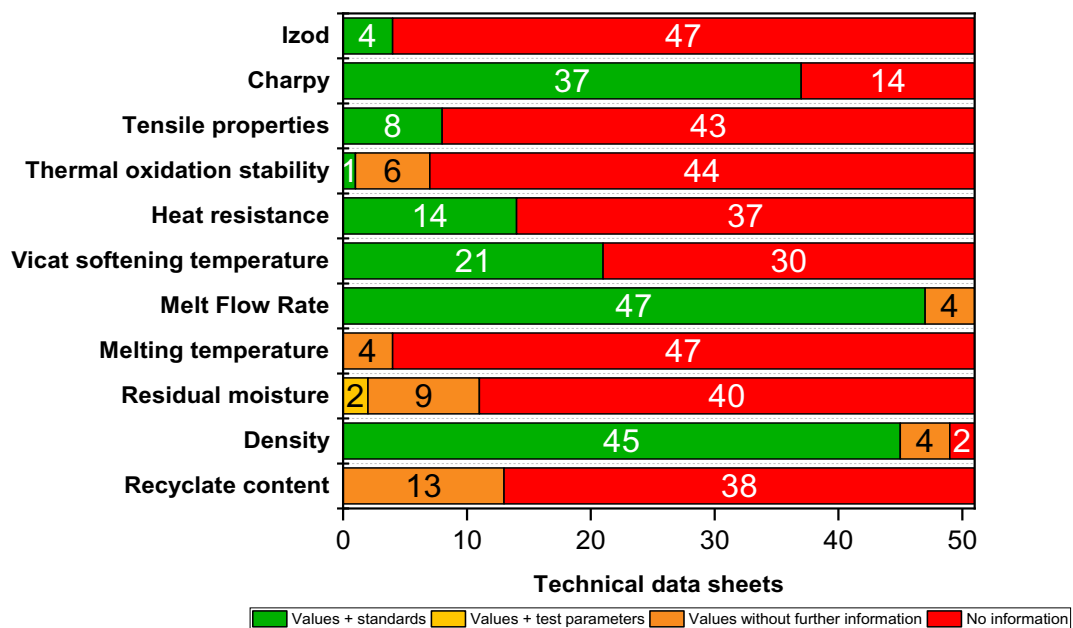


Figure 7: Information on properties of recycled PP from evaluated technical data sheets (Hans-Josef Endres and Madina Shamsuyeva 2020).

The new standard, DIN SPEC 91446, is used to classify plastic recyclates and is intended to provide a clear definition of recyclates and to simplify consistent communication for stakeholders along the entire value chain. Aim of this standard is to leave behind

"PCR flowerpot" qualities and to find a way towards a valuable material for automotive, packaging and construction sectors. Recycled materials should not be inferior to virgin materials in any way, neither in quality nor in quantitative availability. (Fischer 2021).

Another standard regarding long-term application is ONR CEN/TS 14541-2. It deals with plastics pipes and fittings and the utilization of thermoplastics recyclates in that term. According to that standard, it is recommended that quality management plan of the supplier of recyclates is not less strict than corresponding requirements of DIN EN ISO 9001, the internationally known standard for the certification of quality management systems. The standard contains a guideline regarding properties and related test methods suitable for an agreed specification between recyclate supplier and product manufacturer. It states that recycled PP for applications in pipes and fittings must not contain uncoated calcium carbonate, for example. To characterize lifetime under cyclic load of a thermoplastic recyclate, a failure curve by means of cyclic cracked round bar (CRB) test according to (ISO 18489) shall be determined. Failure curves should be based on at least four individual CRB tests with different test loads  $\Delta\sigma$ . This generated failure curve should be included as a reference failure curve in agreed specification for a particular thermoplastic recyclate (Kunststoffrohrverband e.V. - Fachverband der Kunststoffrohr-Industrie 2023). Test parameters in this context for PP are listed in Table 2.

Table 2: Test parameters for cyclic CRB test of polypropylene (ONR CEN/TS 14541-2).

Test frequency	5 Hz
Test loads $\Delta\sigma_{\min} - \Delta\sigma_{\min}$	13 MPa – 16 MPa
Test temperature	$23 \pm 2$ °C
Waveform	sinusoidal
Failure mode	Growth of brittle crack

For quality assurance or iterative batch control of a thermoplastic recyclate, two CRB tests should be performed within the respective range of the test load  $\Delta\sigma$ . Following test outcomes (situation *a*, *b*, *c*) are discussed below and presented in Figure 8. If the number of cycles until failure ( $N_f$ ) in both batch control tests exceeds the corresponding values of the reference failure curve, (as defined in the agreed specification) test is considered to have passed. The material can be considered for further processing (situation *a*). The

individual tests do not necessarily need to be continued until failure and can be terminated before, if the corresponding level is reached.

If in one or both batch control tests  $N_f$  is reached below the corresponding values of the reference failure curve (as defined in the agreed specification) the material failed and is not allowed for further processing (situation *b*, *c*) (Kunststoffrohrverband e.V. - Fachverband der Kunststoffrohr-Industrie 2023).

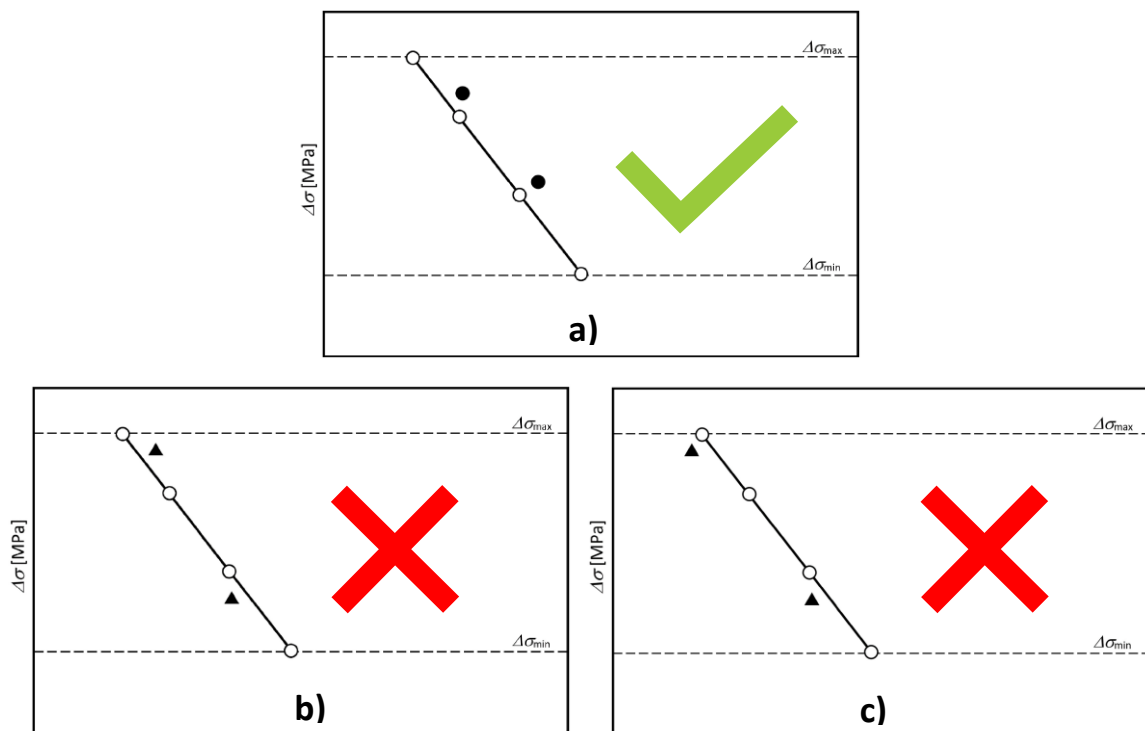


Figure 8: Failure cycle numbers  $N_f$  as a function of the applied stress range  $\Delta\sigma$ , schematic representation of the pass/fail criteria for the cracked round bar test (ONR CEN/TS 14541-2).

### 2.2.3 Circular economy action plan

The European Commission presented in 2015 the “Circular Economy Action Plan”, which identifies priority sectors of plastics, food waste, biomass and bio-based products, critical raw materials, construction and demolition. In 2018, the revised regulatory framework for the circular economy included following key aspects:

- 1) EU recycling target of 65 % of municipal waste by 2035
- 2) EU target for recycling 70 % of packaging waste by 2030
- 3) Binding target to reduce landfilling to a max. of 10 % of municipal waste by 2035



- 4) Ban on landfilling separately collected waste, requiring separate collection of biowaste by 2023 and textiles and household hazardous waste by 2025
- 5) Promotion of economic instruments to discourage landfilling
- 6) Simplified, improved definitions and harmonized calculation methods for recycling rates across the EU
- 7) Concrete measures to promote reuse of materials in industry
- 8) Binding extended producer responsibility schemes for manufacturers to bring greener products to market and support recovery and recycling schemes

Finally, the 2018 EU Strategy for Plastics in a Circular Economy confirms that all plastic packaging should be designed to be recyclable or reusable by 2030. The strategy aims to improve plastic recycling, reduce plastic waste litter, address the plastic value chain and benefit from global action. Council and Parliament decided in 2018 to restrict certain single-use plastic products. Accordingly, single-use plastic cutlery, plastic plates and straws, expanded polystyrene food and beverage containers and plastic cotton swabs will be banned from 2021. Polyethylene terephthalate (PET) beverage bottles must contain at least 25 % recycled plastic from 2025 and at least 30 % from 2030 (Anke Herold et al. 2023).

### **2.3 Fillers and their influence on material properties**

The next paragraphs deal with fillers used in plastics production and processing. It is discussed which types of fillers are intended for which purpose and how they work. Focus is on inorganic fillers such as talc and calcium carbonate ( $\text{CaCO}_3$ ).

Polymer materials are filled by adding a second component to the base material, the matrix. Fillers are solid, inorganic or organic materials, which are dispersed in polymers. Active fillers improve certain mechanical properties and are so called reinforcing fillers. Inactive fillers are usually low-cost fillers such as chalk or talc, which mainly increase the volume while reducing the material price. However, it is not always possible to clearly distinguish between reinforcing or filling materials, since one and the same added component can increase some characteristic values but simultaneously reduce others. Properties such as density, modulus of elasticity, hardness and heat deflection temperature are increased, while decreasing elongation and toughness are compromised for example.

In addition, a lower tendency to shrinkage can be expected, since the filler itself hardly shrinks (Ehrenstein 2011; Bonten 2016).

Reinforcing effects depend on geometry, loading conditions and on general material properties. While a spherical reinforcement increases compression strength and decreases tensile strength, a fiber reinforcement increases tensile and compressive strength. Two-dimensional particles minimize shrinkage but are weakened perpendicular to the plane of the platelet. Talc, for example, is 2-dimensionally plate-like, whereas chalk is three dimensionally distributed in the matrix (Ehrenstein 2011). The best balance of processability, mechanical properties, aspect ratio and costs is shown by talc (J. Schöne et al. 2012).

### **2.3.1 Talc**

Talc is a layered silicate that occurs naturally in great abundance. Other common names are magnesium silicate hydrate, steatite or soapstone. Talc has been known since ancient times, and there are far more than 2000 occurrences of it worldwide. It is a soft mineral and easily micronizable into fine particle sizes. Powdered talc has a wide range of applications and, due to its versatile properties, serves as one of the most important fillers for polymers (Cosmacon 2022).

The fine plate-like particles of talc efficiently fill up inter-particle spaces within polymer compounds which leads to better mechanical properties of the material. Talc has better thermal conductivity compared to polymers. This means that an addition of talc increases heat transfer through the compound. As a result, both processing and cooling of plastic compounds is accelerated by talc, leading to faster manufacturing rates. Polymers filled with fine and lamellar talc are able to withstand higher elongations without deformation compared to unfilled polymers. In addition, talc achieves the highest creep resistance compared to all other mineral fillers. Because of talc's lamellar structure, combined with its fineness it fills the smallest pores in a polymer which prevents water vapor or oxygen from penetrating through the resulting products. This property is crucial for the food and pharmaceutical packaging industries. Due to its hydrophobicity (water-repellent property) and chemical inertness, talc contributes to the chemical resistance of plastics and polymers (Avani Group of Industries 2020).

Referring to PP, the addition of fillers is a common way to improve material properties and/or save costs. An addition of talc is known to improve properties of PP, such as strength, dimensional stability, stiffness and crystallinity, but it has a negative effect on other properties, like impact strength and formability (Bakar et al. 2007; Lapcik et al. 2009). Depending on the amount and size of talc particle added, the compound behaves differently. (Ammar O et al. 2017b). At low concentrations (less than 3 weight %), talc acts as a nucleating agent, reducing spherulite size and shortening processing time (Fillon et al. 1994). At higher contents (10 - 40 wt %), it acts as a reinforcing filler, increasing tensile modulus and stiffness but reducing elongation at break as well as impact strength (Maiti and Sharma 1992). The reinforcing capacity of talc as a filler depends on the surface activity, particle size, surface area and surface functional groups (Sinha Ray et al. 2002; McLauchlin and Thomas 2009).

Regarding crack initiation and crack propagation talc also has an influence on PP. The impact on crack resistance varies with the amount used as well as the quality of the talc. Higher talc content and lower talc quality (larger particle size) reduces the material's plastic deformation ability and toughness (J. Schöne et al. 2012). According to (Florian J. Arbeiter et al. 2016) talc reinforcement changes the failure behavior in CRB tests significantly. Fibrils are formed between mineral reinforcement particles what can be addressed to the polymer matrix. Quasi-brittle failure shows a shallower slope in CRB test, compared to the unreinforced material, which could be useful for application with low stress levels (see Figure 9).

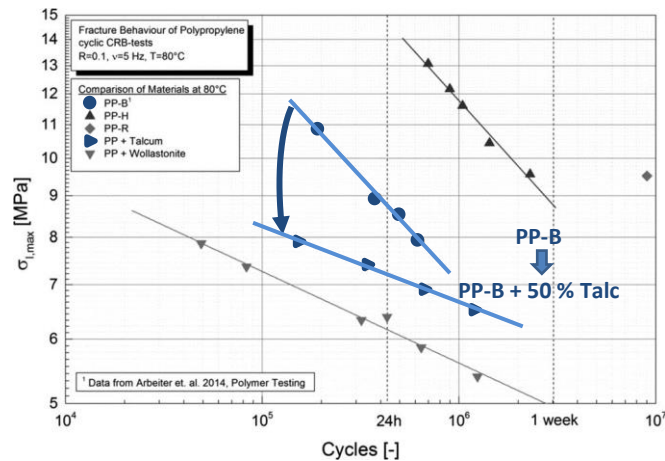


Figure 9: Results of cracked round bar (CRB) test of talc filled (triangle) and non-talc filled (circle) PP, tested at 80 °C in quasi-brittle failure mode (Florian J. Arbeiter et al. 2016).

### 2.3.2 Calcium carbonate

Calcium carbonates ( $\text{CaCO}_3$ ) are one of the most common minerals in the earth's crust. They occur in the form of limestone and chalk, formed from fossils, and marble, formed by the metamorphism of sedimentary rocks. They are composed largely (> 98 %) of  $\text{CaCO}_3$ , with some traces of magnesium carbonate, iron oxide, and aluminum silicates. All minerals are relatively soft and are white in color. (Maier and Calafut 1998). Calcium carbonate is the most commonly used filler in polymer formulations. It is inexpensive and can be used in high amounts. Generally, it is used as extender, but at the same time it is able to improve stiffness and impact strength.

Regarding PP, too high  $\text{CaCO}_3$  content reduces strength to a value below that of pure PP. Yield strength ( $\sigma_Y$ ) is also lowered with increasing filler content which is explained by debonding of particles from the PP matrix. (Maier and Calafut 1998; Martín-Martínez and José Miguel 2002; Yanwei Jing et al. 2018; W.C.J Zuiderduin et al. 2003).

Because of a high degree of gloss and brightness  $\text{CaCO}_3$  is frequently used in PP products (e.g. packaging applications). Disadvantages include lower tensile and compressive strength and strongly reduced elongation at break. The mineral is available in various grades. Surface-treated grades are coated with lipophilic substances such as stearic acid or calcium stearate. This improves dispersibility, tensile strength, flexural strength, modulus, crystallization property and oxidation resistance of the filled resin but leads to a decrease in

impact strength. It is known as nonabrasive filler, resulting in a reduction of abrasion on processing machinery. In experimental tests, coated CaCO<sub>3</sub> showed higher impact strength, elongation at break ( $\epsilon_B$ ) and better whiteness compared to uncoated grades (Maier and Calafut 1998; Mallick 2006; Yanwei Jing et al. 2018; Mallick 2006).

### 3 EXPERIMENTAL

The experimental chapter is divided in two parts. At the beginning, the batch variation under investigation is presented. The second part deals with standard characterization techniques to generate a basic material analysis with additional approaches to investigate lifetime under cyclic load by means of cyclic CRB test.

#### 3.1 Material selection

This thesis aims to monitor the influence of batch variations of PCR - PP on relevant material properties. All materials were provided by the same company as depicted in Figure 10. In the following batch 1 is referred to as B1 and continuing.



Figure 10: Batches under investigation, time interval from August, 2021 to November, 2022.

Additionally, B2 and B5 were mixed with a virgin polypropylene (vPP), more precisely a PP block copolymer (which is used in pipe extrusion) in a ratio of 75 % to 25 % (vPP/B). The material blends are referred to as M1 and M2 respectively (see Figure 11). Goal was to investigate the influence PCR - PP has on a vPP regarding lifetime under cyclic loading and whether the vPP eliminates possible material variations.

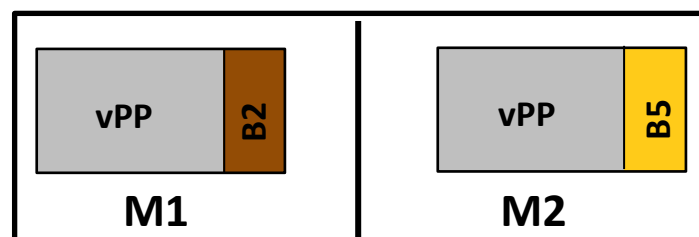


Figure 11: Material blend M1 and M2.

For the two blends, resin of vPP and of B2, respectively B5 were compounded. Regarding cyclic CRB test specimens for all ten batches as well as M1 and M2 were processed out of compression molded sheets according to ISO 18489.

To perform several test procedures samples were cut out of multipurpose specimens which were processed for each supplied batch. Those multipurpose specimens were injection molded on an injection molding machine from type Allrounder 320C (Arburg, Loßburg, Germany), provided with a screw of 20 mm in diameter and a maximum clamping force of 50 tons. The machine was equipped with a single-cavity tool for the production of multipurpose specimens. Parameters for injection molding process are given in Table 3.

Table 3: Parameters of injection molding.

Hopper temperature	[°C]	30	Back pressure	[bar]	30
Temperature cylinder 1	[°C]	190	Injection pressure	[bar]	920
Temperature cylinder 2	[°C]	210	Holding pressure	[bar]	900
Temperature cylinder 3	[°C]	220	Holding pressure time	[s]	16
Temperature cylinder 4	[°C]	230	Switch-over point	[cm <sup>3</sup> ]	12
Nozzle temperature	[°C]	230	Melt cushion	[cm <sup>3</sup> ]	10,5
Mold temperature	[°C]	40/40	Residual cooling time	[s]	50
Injection speed	[cm <sup>3</sup> /s]	20	Cycle time	[s]	70

### 3.2 Material characterization and test methods

Following paragraphs provide a concise introduction of applied testing methods to obtain an overall impression of the batch variation. Specifically, standard test methods, namely density, melt flow rate (MFR) melt volume rate (MVR), differential scanning calorimetry (DSC), oxidation onset temperature (OOT), thermogravimetric analysis (TGA), and Fourier transform infrared spectroscopy (FTIR) were carried out, as well as tensile and Charpy impact tests. Furthermore, rheometric tests and dynamic mechanic analysis (DMA) were performed by the Vienna University of Technology (TU Wien). In addition to the standard test methods for material characterization lifetime under cyclic load, by means of cyclic CRB test, were carried out.

### 3.2.1 Density

Density of the batches was measured using a balance of the type Mettler Toledo XS205 Dual Range (Mettler-Toledo GmbH, Greifensee, Schweiz) according to ISO 1183-1. For each material samples were cut out of multipurpose specimens. Sample mass was determined in air and in an auxiliary liquid, which was distilled water with a known density at different temperatures. Five samples per material were measured and the mean value was used for further evaluation. Density was calculated with Equation (1).

$$\rho_i = \frac{m_{Air,i} \cdot \rho_{Water}(T)}{m_{Air,i} - m_{water,i}} \quad (1)$$

$\rho_i$	density of polymer i
$m_{Air,i}$	mass of polymer I measured in air
$m_{Water,i}$	mass of displaced water by polymer i
$\rho_{Water}(T)$	density of water as a function of temperature

### 3.2.2 Melt flow rate

The MFR is commonly used in industry as an entrance or exit quality control as it provides a quick indication of the materials flowability. Viewed from the rheological aspect it marks a single-point value of a material's viscosity. A sample is heated in a cylinder to a temperature above  $T_m$  for semi-crystalline thermoplastics. The molten material is pressed through the capillary by a piston with a standardized temperature and weight for the respective material. In case of PP it is 230 °C and 2.16 kg. For this thesis a device from type MFI ITW Instron CEAST (Pianezza, Italien) was used to determine MFR. Nozzle dimensions are  $\varnothing$  2.095 mm in diameter with a length of 8.0 mm.

Determination of MFR is standardized in (ISO 1133) and defined as amount of material in grams that flows through a capillary under a defined pressure and temperature in ten minutes [g/10 min] (Grellmann and Altstädt 2011). The easier the flow, the higher the MFR. It is evaluated using equation (2) (ISO 1133).

$$MFR = \frac{m \cdot 600}{t} \quad (2)$$

t	cut-off interval time [s]
m	mass of polymer output in cut-off interval [g]



Simultaneously the average MVR value was determined by the device. It is defined as volume of a material that flows through a capillary with a defined pressure and temperature in ten minutes [ $\text{cm}^3/10 \text{ min}$ ]. With the MVR it is possible to eliminate the influence of melt density (Grellmann and Altstädt 2011). Further, density was calculated corresponding to the values of the melt flow/volume rate with equation (3).

$$\rho = \frac{MFR}{MVR} \quad (3)$$

$\rho$	density [ $\text{g}/\text{cm}^3$ ]
MFR	Melt flow rate [ $\text{g}/10 \text{ min}$ ]
MVR	Melt volume rate [ $\text{cm}^3/10 \text{ min}$ ]

### 3.2.3 Rheometric experiments

Rheological analysis is important for a deeper understanding of flow behavior, deformation of materials under force application and viscoelastic properties. The relationship between shear stress and shear rate, that actually defines flow behavior of a polymer melt, is determined by means of rheometry. For this purpose, various test setups are available. In course of this thesis, a rotational plate-plate rheometer was used which is characterized by two plane-parallel plates with radius ( $R$ ) and distance ( $H$ ). Velocity gradient in this measuring arrangement depends on  $R$  of the rotating upper plate and the height of the gap. It allows variation of the shear rate over a wide range by changing the plate spacing or angular speed. (Grellmann 2011). The geometry of a typical test setup is depicted in Figure 12.

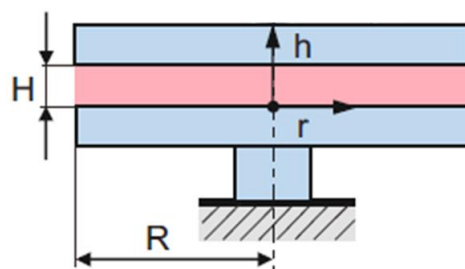


Figure 12: Geometry of a plate-plate rheometer (Grellmann 2011).

These measurements were carried out at Vienna University of Technology using a rheometer from type MCR 302 (Anton Paar GmbH, Austria) at a temperature of  $230 \text{ }^\circ\text{C}$ , according to (DIN EN ISO 3219-2). Zero viscosity was measured in oscillation mode, storage

modulus ( $G'$ ) and loss modulus ( $G''$ ) in rotation mode. Nitrogen was used as purge gas. Samples were melt-pressed into 1.2 mm thick circular disks with a diameter of 25 mm. Zero viscosity was determined at a shear rate of  $0.001 \text{ s}^{-1}$ . Furthermore, the “cross over” point was determined. It is defined as the intersection of  $G''$  and  $G'$  (Frick 2011).

### 3.2.4 Thermal analysis

In order to characterize and compare materials and to make predictions of certain properties, DSC measurements are routinely performed. In the frame of this thesis all measurements were carried out on a DSC 4000 of PerkinElmer (Waltham, Massachusetts, USA). Nitrogen with a flow rate of 50 ml/min functioned as purge gas. Samples were heated using a heating rate of  $10.00 \text{ }^\circ\text{C}/\text{min}$  for DSC (DIN EN ISO 11357-1).

Results were evaluated using the Pyris Manager<sup>®</sup> software (PerkinElmer, Waltham, Massachusetts, USA). With DSC the crystallite  $T_m$  and melting enthalpy ( $\Delta H_m$ ) were determined. The heat flow  $dQ/dt$  to a test specimen compared to a reference (empty crucible) is used as the measured quantity (Grellmann and Altstädt 2011).

There are different methods to determine the degree of crystallinity out of a DSC heat flow curve. The simplest and most widely used approach involves integrating the area of a crystallization or melting peak to determine the  $\Delta H_m$  of a material, schematically shown in Figure 13.

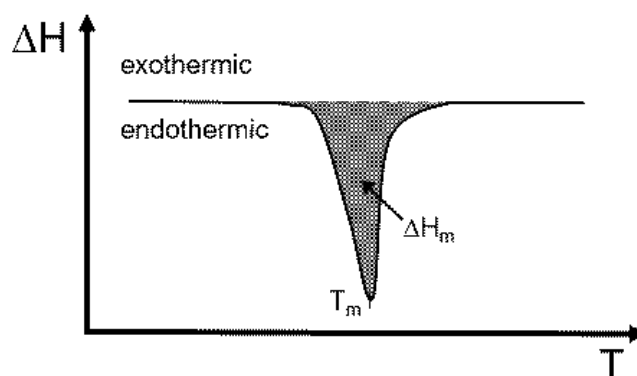


Figure 13: Enthalpy change  $\Delta H_m$  for semi-crystalline thermoplastics at constant heating rate above glass transition region, determination of crystallite melting temperature  $T_m$  (Ehrenstein et al. 2003).

In Equation (4)  $D$  is calculated as the ratio between  $\Delta H_m$  and its equilibrium melting enthalpy a melting enthalpy of a theoretically 100 % crystalline material ( $\Delta H_m^0$ ). For PP,  $\Delta H_m^0$  is 207 J/g, respectively, 293 J/g for PE (Ehrenstein et al. 2012).

$$D = \frac{\Delta H_m}{\Delta H_m^0} [\%] \quad (4)$$

For batches with pronounced PE impurities, melt enthalpy was determined with the method shown in Figure 14: Schematic DSC curve showing applied method for separate calculation of enthalpy  $\Delta H_{m,PE}$ , and  $\Delta H_{m,PP}$  Figure 14. Using Pyris Manager® software, the total area of both peaks was evaluated (green) and afterwards the area of PE (blue) was subtracted, treating the remaining area as  $\Delta H_m$  of PP.

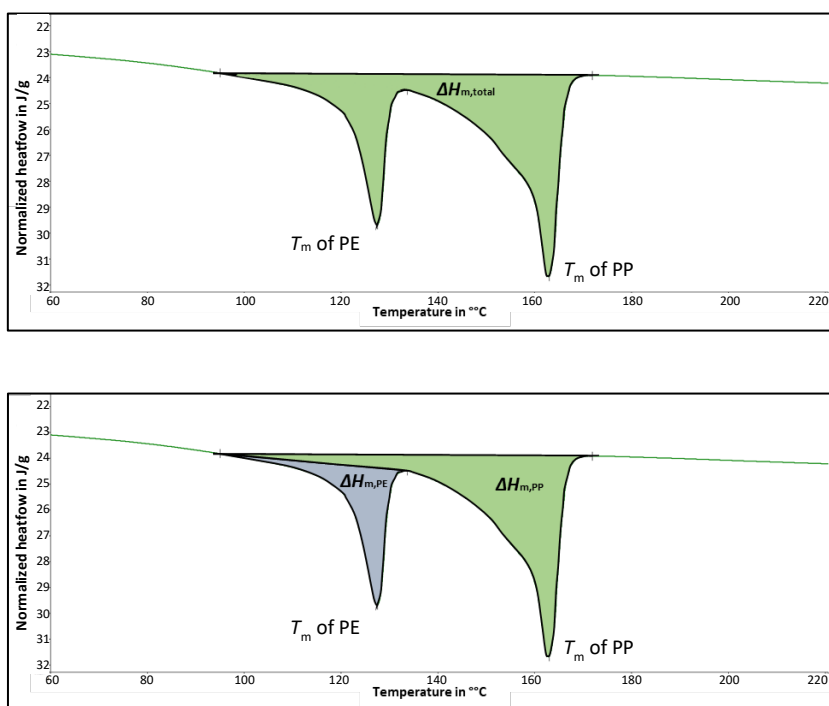


Figure 14: Schematic DSC curve showing applied method for separate calculation of enthalpy  $\Delta H_{m,PE}$ , and  $\Delta H_{m,PP}$

To gain information about stabilizer activity OOT was determined. For this measurement a sample is exposed to a gaseous oxidant (oxygen or synthetic air) at an elevated temperature.

For the execution of OOT measurements the dynamic method was applied, where the specimen is heated 20.00 °C/min (ISO 11357) in an oxygen or air atmosphere with a flow of 50 ml/min from the very beginning of the process (Ehrenstein et al. 2012).

### 3.2.5 Thermogravimetric analysis

With TGA the mass or mass change of a sample as a function of temperature, time or both is measured. Mass changes occur during sublimation, evaporation, decomposition, chemical reactions as well as magnetic or electrical transformations.

A TGA curve is a direct way of describing an endothermic process with mass loss (evaporation) and without mass loss (melting). The change in mass of a sample is measured either absolutely in milligrams or relatively as percentage of initial mass and plotted against temperature or time. Plastics can change their mass in one (see Figure 15) or more steps.

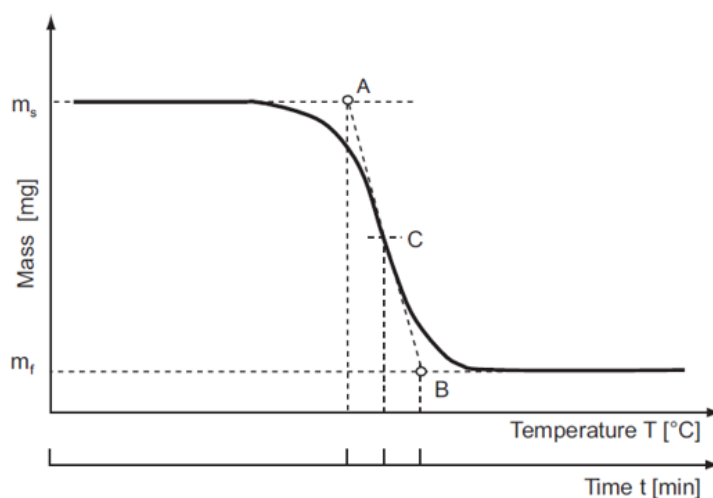


Figure 15: Typical TGA curve with single step mass loss.

$m_s$  Mass before heating

$m_f$  Mass after end temperature attained

A Starting point (Intersection of extrapolated starting mass with the tangent applied to the maximum slope)

B End point (Intersection of extrapolated end mass after reaction with the tangent applied to the maximum slope)

C Midpoint (Intersection of the TG curve with the line parallel to the abscissa that is midway between A and B)

Crucial factors are choice of purge gas and conditions in the sample chamber. The extent of heat transfer to a sample depends on the gas flow rate. In the frame of this work, nitrogen served as inert purge gas with a flow rate of 20 ml/min. The sample was heated from 35 °C up to 850 °C using a heating rate of 10 °C/min. (Ehrenstein et al. 2012). Three samples for each batch were prepared and measured on a TGA 8000 of PerkinElmer

(Waltham, Massachusetts, USA). Results were analyzed using Pyris Manager® software (PerkinElmer, Waltham, Massachusetts, USA). Due to technical problems batch 7-9 were measured on another device (TGA/DSC 3+, Mettler-Toledo GmbH, Greifensee, Schweiz). But reference measurements of already measured batches were performed and checked, to ensure that comparability is given.

### 3.2.6 Dynamic mechanic analysis

The DMA is an important technique for measuring mechanical and viscoelastic properties of polymers. In DMA, a specimen is subjected to a periodic load in one of several deformation modes (bending, tension, shear, and compression). The modulus is measured as a function of time or temperature and provides information on phase transitions (Mettler-Toledo Inc. all rights reserved 2022).

Due to the viscoelastic material behavior, there is a time shift between load and deformation, which can be recognized as a phase shift of the two vibrations. Thus, from equation (5) to (8) the complex modulus  $E^*$ , the storage modulus  $E'$  and the loss modulus  $E''$ , as well as the loss factor  $\tan\delta$  can be calculated. In equation (3)  $\varepsilon_A$  is the strain as a deflection and  $\sigma_A$  the stress as step response (Ehrenstein et al. 2012).

$$|E^*| = \frac{\sigma_A}{\varepsilon_A} \quad (5)$$

$$|E^*| = \sqrt{(E')^2 + (E'')^2} \quad (6)$$

$$E^* = E' + i * E'' \quad \text{with } i = \sqrt{-1} \text{ as imaginary unit} \quad (7)$$

$$\tan\delta = \frac{E''}{E'} \quad (8)$$

In context of this work, DMA measurements were carried out by means of 3 – point bending deformation mode in a temperature range of -50 °C to 150 °C with a DMA Q800 (Anton Paar GmbH, Graz, Austria).

### 3.2.7 Fourier Transform Infrared Spectroscopy

One of the most efficient and fastest techniques for detecting differences between different polymers is FTIR (Grellmann 2011). For all measurements, FTIR coupled with

Attenuated Total Reflectance (ATR) mode was applied in preference to transmission mode using a SpectrumTwo spectrometer developed by PerkinElmer (PerkinElmer, Waltham, Massachusetts, USA). It is equipped with a ZnSe window and a single reflection diamond (UATR).

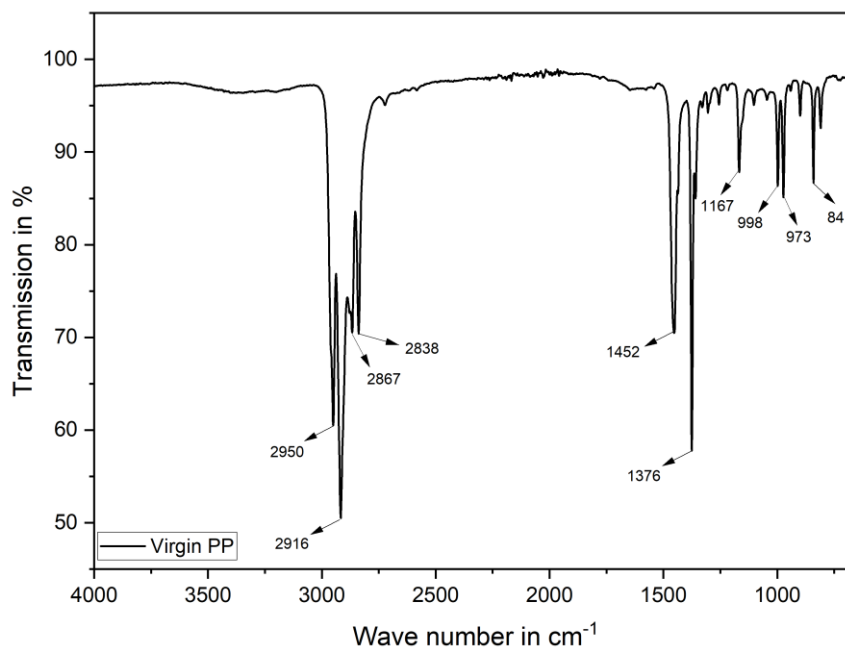


Figure 16: FTIR spectra of virgin polypropylene (PP).

Four scans were accumulated per spectrum in a range of 4000 cm<sup>-1</sup>–650 cm<sup>-1</sup> with a resolution of 4 cm<sup>-1</sup>. Ten FTIR spectra were recorded for each batch from multiple sections of a standard multipurpose specimen. Percentage of transmittance (or absorbance) at characteristic peaks was evaluated with Spectrum<sup>®</sup> software.

Figure 16 shows a representative spectrum of standard PP. Characteristic absorption bands are listed in

Table 4 including the main active group vibrations of PP which are stretching, bending, rocking or wagging. Transmission peaks long from “very very strong” to “medium” for PP. As talc and chalk (CaCO<sub>3</sub>) are the most commonly used filler for polymers, FTIR-ATR spectra of both is presented in Figure 17. Pronounced peaks for talc are at a wave number of 3673 cm<sup>-1</sup> and in a range from 1062 cm<sup>-1</sup> to 254 cm<sup>-1</sup>, for chalk instead, at 1394 cm<sup>-1</sup> and 871 cm<sup>-1</sup>, respectively 712 cm<sup>-1</sup>.

Table 4: Main active group vibrations of polypropylene (b = backbone, m = medium, s=strong, v = very,  $\delta$  = bending,  $\nu$  = stretching,  $\rho$  = rocking,  $\omega$  = wagging (Andreassen 1999).

Vibration type	Wave number [cm <sup>-1</sup> ]
$\nu$ CH <sub>3</sub> asym	2950 vvs
$\nu$ CH <sub>2</sub> asym	2916 vvs
$\nu$ CH <sub>2</sub> sym	2867 vs
$\nu$ CH <sub>2</sub> sym	2838 vs
$\delta$ CH <sub>3</sub> asym., $\delta$ CH <sub>2</sub>	1452 s
$\delta$ CH <sub>3</sub> sym., $\omega$ CH <sub>2</sub> , $\delta$ CH, $\nu$ CC <sub>b</sub>	1376 s
$\nu$ CC <sub>b</sub> , $\rho$ CH <sub>3</sub> , $\delta$ CH	1167 m
$\rho$ CH <sub>3</sub> , $\delta$ CH, $\omega$ CH <sub>2</sub>	998 m
$\rho$ CH <sub>3</sub> , $\nu$ CC <sub>b</sub>	973 m
$\rho$ CH <sub>2</sub> , $\nu$ CC <sub>b</sub> , $\nu$ C-CH <sub>3</sub> , $\rho$ CH <sub>3</sub>	841 m

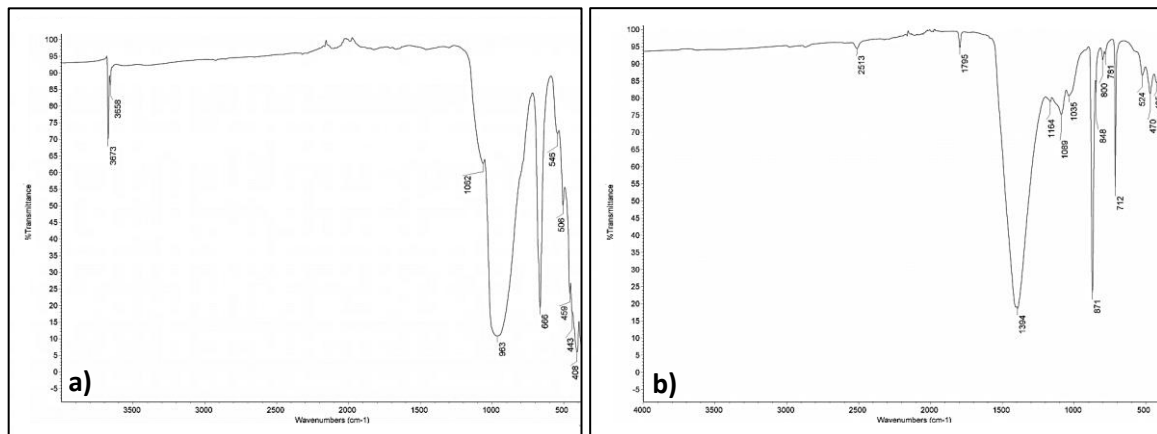


Figure 17: a) Spectrum of talc (University of Tartu 2023a) , b) Spectrum of chalk (University of Tartu 2023b).

### 3.2.8 Tensile test

Tensile test is applied to characterize the stress-strain ( $\sigma - \epsilon$ ) behavior of a material with the aim of determining characteristic values such as Young's modulus  $E$ , yield strength  $\sigma_Y$  and elongation at break  $\epsilon_b$  (Grellmann 2011).

Tensile properties of the batches under investigation were determined according to (ISO 527). Therefore, five specimens of each material were measured and evaluated using a tensile/compression universal testing machine of type Z010 (ZWICK GmbH & Co. KG, Ulm,

Germany) with a 10 kN load cell at room temperature ( $T = 23 \text{ }^\circ\text{C}$ ). Up to the yield stress, strain is measured by makro detectors (makroXtens II, ZwickRoell GmbH & Co. KG, Ulm, Germany) and after that via machine crosshead. Makro positioning is depicted in Figure 18. For a precise evaluation, Young's modulus was determined with makro detectors at a test speed of 1 mm/min. Subsequently, the measurements are carried out at a test speed of 50 mm/min until failure.



Figure 18: Makro positioning on multipurpose specimen, tensile test setup.

### 3.2.9 Charpy impact test

Charpy impact test is a method to determine impact strength and notched impact strength of materials. Notched impact strength of materials is of particular technical relevance, since notches frequently occur in structural parts (surface defects, ribs, edges, etc.). In accordance with (ISO 179-2) a Zwick HIT25P (ZwickRoell GmbH & Co. KG, Ulm, Germany) with an instrumented pendulum was used.

For Charpy arrangement, the notch side of a specimen is centered on two abutments. Samples were made from injection molded standard multipurpose specimens (see Table 3). For each batch ten notched and ten unnotched specimens were tested. The set nominal working capacity was 2 J for notched respectively 15 J for unnotched samples. The machine detected absorbed energy during impact and the fracture was analyzed and determined by naked eye. To evaluate Charpy impact strength  $a_{cU}$  of unnotched specimens, impact energy consumed  $W_c$  is related to the initial cross section of the test specimen, calculated as follows in equation (9) (Grellmann 2011).

$$a_{cU} = \frac{W_c}{b \cdot h} \quad (9)$$



- b width of specimen [m<sup>2</sup>]  
 h height of specimen [m<sup>2</sup>]

To determine Charpy notched impact strength  $a_{cN}$ , a notched test specimen is positioned centrally on the support and the notch is located on the tensile side. Consequently, impact is applied to the opposite side of the notch. Charpy notch impact strength  $a_{cN}$  is calculated from impact energy  $W_c$ , related to the smallest initial cross-section of the test specimen at notch base  $b_N$  using equation (10) (Grellmann 2011).

$$a_{cN} = \frac{W_c}{b_N \cdot h} \quad (10)$$

- $b_N$  residual width of specimen at notch bottom [m<sup>2</sup>]

The difference between impact strength  $a_{cU}$  and notched impact strength  $a_{cN}$  provides information about sensitivity of a polymer material to external notches. It is possible to determine a notch sensitivity from the quotient of  $a_{cN}$  and  $a_{cU}$ , specified in equation (11) (Grellmann 2011).

$$k_z = \frac{a_{cN}}{a_{cU}} \cdot 100\% \quad (11)$$

- $k_z$  notch sensitivity [%]

### 3.2.10 Lifetime under cyclic load via CRB test

Additional to the standard test methods for material characterization, measurements on long-term performance by means of cyclic CRB test were carried out according to (ISO 18489).

The CRB test is one main approach to characterize lifetime under cyclic load. Specimens were tested at an ambient temperature of 23 °C on a servo-hydraulic actuator system (MTS Systems GmbH, Berlin, Germany). To prevent hysteretic heating of PP, testing frequency  $f$  was reduced to 5 Hz and the ratio of minimum to maximum stress ( $R$ -ratio) was kept constant at 0.1. For each batch at least six specimens were tested at different stress levels until total failure. The applied stress level  $\Delta\sigma_0$  was varied from  $\Delta\sigma_0 = 8,5$  MPa up to  $\Delta\sigma_0 = 15$  MPa to reach failure at a cycle number between  $N_f = 10^4$  and  $3 \cdot 10^6$  cycles.

For further characterization of fracture surfaces of CRB specimens, optical microscopy of type Axioscope 7 (Carl Zeiss AG, Jena, Germany) and scanning electron microscopy (SEM) of type Tescan-Vega-II (Tescan GmbH, Dortmund, Germany) were used. Images via SEM were taken near the notch, in the center of the specimens and in the region of residual fracture. A schematic overview is given in Figure 19.

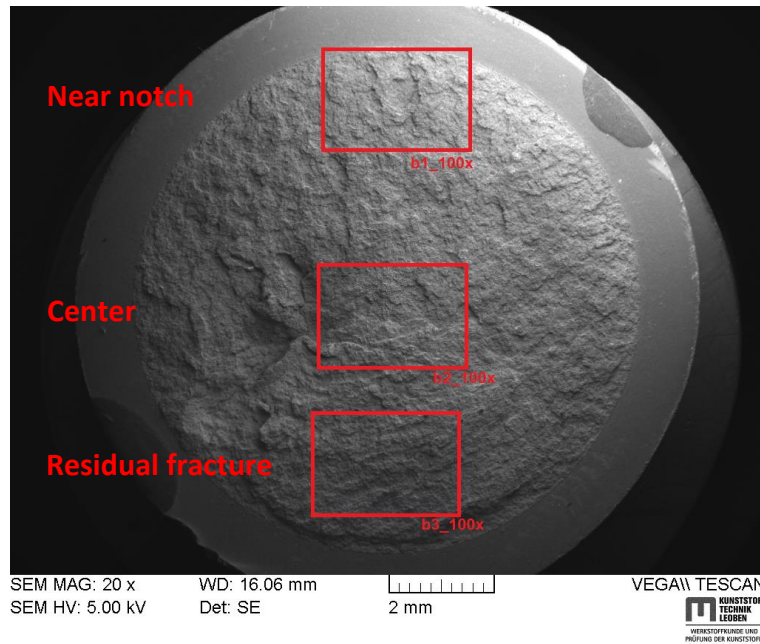


Figure 19: Different regions of SEM images taken.

## 4 RESULTS AND DISCUSSION

This chapter is divided into three parts. First section presents results of basic characterization techniques for the batches. Following, a more in-depth analysis of the long-term behavior via cyclic CRB test of the batches is carried out. Finally, results are summarized and discussed, trying to find correlations between lifetime under cyclic load and other characteristic material properties of the batches under investigation. Necessary data was calculated with Microsoft Excel and subsequently processed with Origin lab® software.

### 4.1 Density

Density was measured in two ways, with a balance and by calculating the quotient of MFR and MVR which led to melt density. Results are depicted in Figure 20 for all batches.

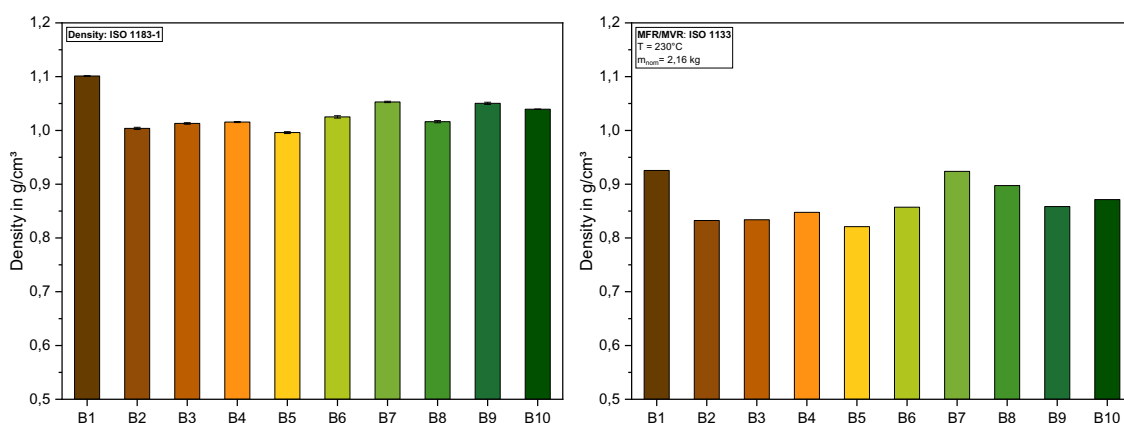


Figure 20: Density measured by balance (left), melt density (right).

Results for melt density (B) show lower values than those measured by balance. In the case of semi-crystalline plastics, the density is determined by the microstructure state. Intermolecular interaction forces in crystalline phases are much larger than in amorphous regions due to a much denser packing of the macromolecules. With increasing packing density (higher degree of crystallinity), the density increases. When heat is applied the intermolecular bonding forces are no longer sufficient, which leads to a melting of the crystalline regions. This is associated with a dissolution of their crystalline orders. So, density of a polymer melt is always lower since it is not as densely packed because it exists

in an amorphous phase. The scattering of the results be explained by the presence of fillers (e.g. talc and calcium carbonate) (Frick 2011). The highest density was determined for B1.

## 4.2 Rheological analysis

In Figure 21 results for all batches are depicted. Lowest values for MFR occur for B2 and B1, with 6 g/10 min respectively 7 g/10 min. Maximum value occurs for B3 with 12 g/10 min. Same appears for the MVR, B2 with 7 cm<sup>3</sup>/10 min respectively, B1 with 8 cm<sup>3</sup>/10 min and the maximum was again reached by B3 with 14 cm<sup>3</sup>/10 min. Trend of MVR is the same as for MFR except results for B5. The MFR of B5 is below B7 and B8 where MVR for B5 is higher than MVR of B7 and B8. This this phenomenon may result from measurement inaccuracies. It should be noted that MFR values spread over a range from 6 g/10 min (B2) to 12 g/10 min - the double.

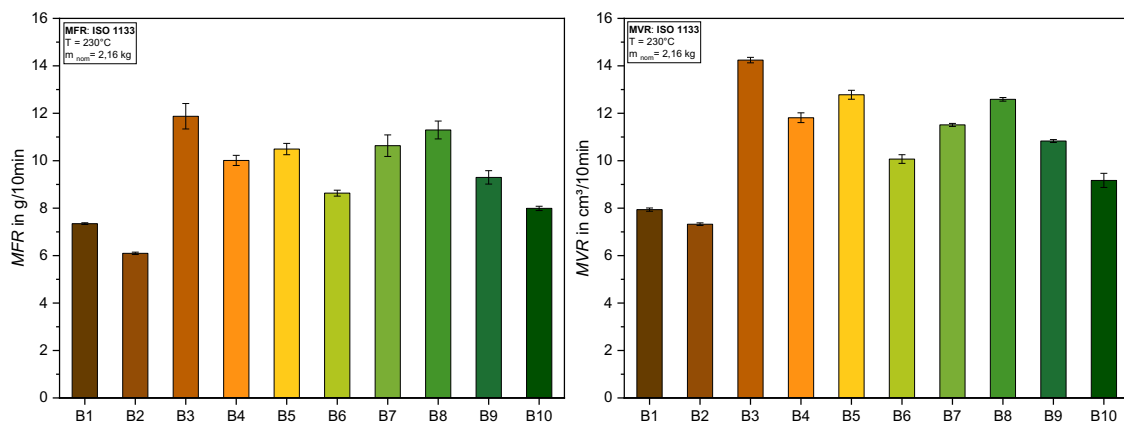


Figure 21: Left: Melt flow rate (MFR), right: Melt volume rate (MVR), both measured at 230 °C with 2.16 kg.

Since MFR values just express one single point on a material's viscosity curve, plate-to-plate rheological measurements were carried out, providing a broader view (Figure 22). At high shear rates (above 10 rad/s) deviations are small compared to the zero-shear viscosity (measured at 0.001 rad/s) where especially B1 excels with 7000 Pas. All other batches are clearly below 3500 Pas. Also curve shape for B1 is different compared to the rest. Viscosity is proportional to the molecular weight, meaning the higher the molecular weight the higher the viscosity (Grellmann 2011).

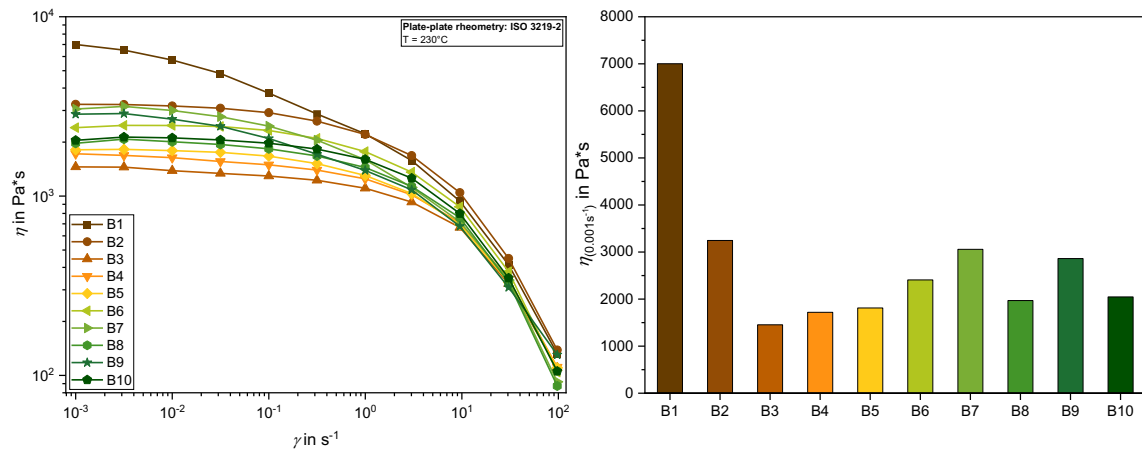


Figure 22: Plate-plate rheometer; T=230 °C, left: shear viscosity  $\eta$  as a function of shear rate  $\gamma$ , right: shear viscosity  $\eta$  at a frequency of  $\omega = 0,001$  rad/s.

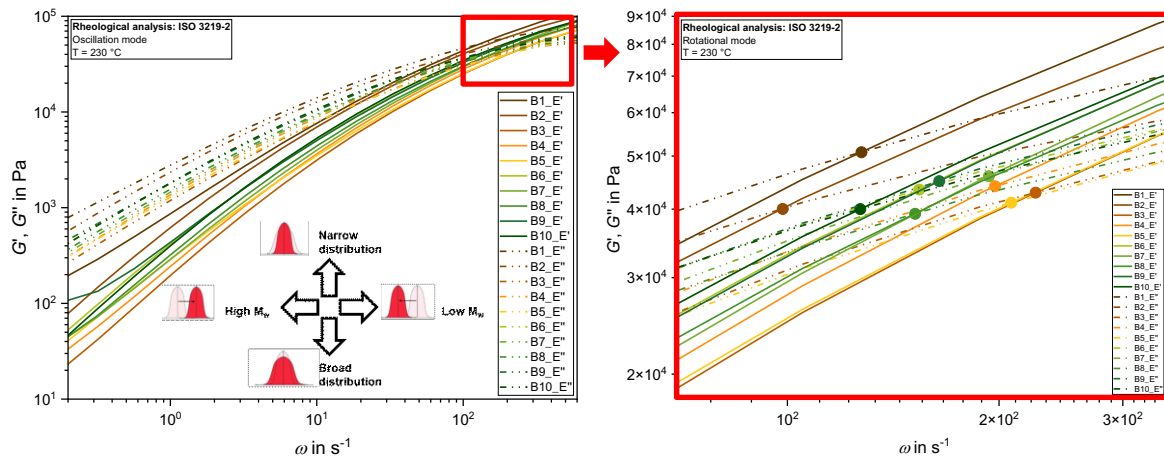


Figure 23: Storage modulus  $G'$  and loss modulus  $G''$  over shear rate  $\gamma$ , determination of cross over point.

In Figure 23 determination of the cross-over point is depicted. It increases more rapidly with increasing frequency and exceeds  $G'$  at a certain frequency. If the cross over point occurs at higher frequencies it means a material has a lower  $M_w$  and if the cross over point is at a higher modulus level it is a sign for narrow distribution of  $M_w$  (Figure 23).

Accordingly, B2 would have the highest  $M_w$  and B3 the lowest. If the cross over point of B6 is taken as reference (middle of data cloud)  $M_w$ , respectively its distribution behaves as follows in Table 5.

Table 5: Molecular weight and distribution with B6 as reference

<b>Batch</b>	<b><math>M_w</math></b>	<b><math>M_w</math> distribution</b>
1	↑↑	very narrow
2	↑↑↑	broad
3	↓↓↓	broad
4	↓↓	narrow
5	↓↓↓	broad
<b>6</b>	<b>REFERENCE</b>	
7	↓↓	narrow
8	↑	very broad
9	↓	narrow
10	↑↑	broad

### 4.3 Thermal analysis

In Figure 24 one representative thermograph via DSC for each batch is depicted. Considering peak temperature, all batches show the for PP typical  $T_m$  at  $\sim 165$  °C with exception of B5, where  $T_m$  is around 162 °C. But B5 shows relatively high scatter compared to the rest. Deviations of this magnitude are normal and can be attributed to sample preparation, for example. It was observed that, with the exception of B6, all batches show a small peak around 125 °C. These peaks are most pronounced for B5, B7 and B9. For these three batches the PE peak was evaluated separately as described in Figure 14 (chapter 3.2.4).

Peaks at 125 °C possibly indicate a small amount of PE in the batches (Furukawa et al. 2006; Strömberg and Karlsson 2009). However, due to small intensity, it may also originate from sufficiently long and thus crystallizable ethylene sequences in PP copolymers (Feng et al. 1998). Such sequences are typically found in block copolymers (Feng et al. 1998; Freudenthaler et al. 2022). In contrast, B6 is the only batch with a peak at 182 °C. The additional peak occurring for B6 could indicate a polyoxymethylene homopolymer (POM-H) impurity (Grellmann 2011).

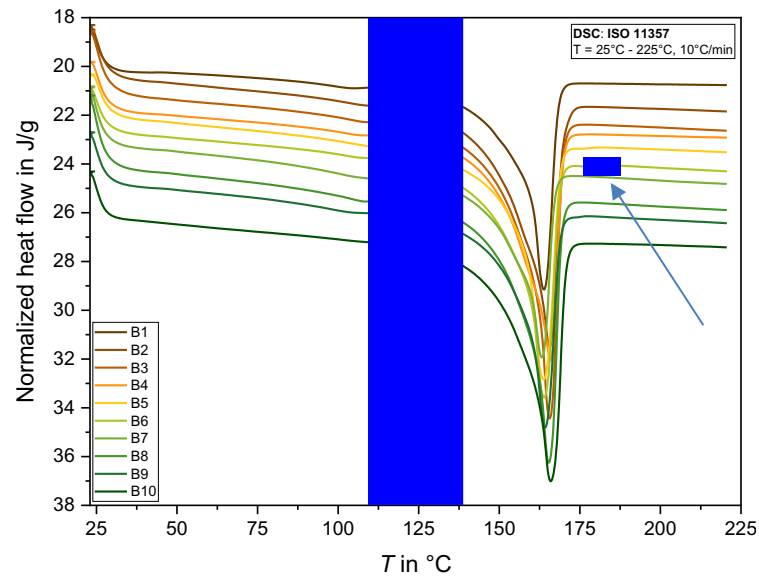


Figure 24: Heat flow  $\dot{Q}_n$  over temperature  $T$  of the second heating curves.

However, the amount is not that significant respectively, noticeable in other measurements, that it would affect other material properties. Results for  $T_m$  and crystallinity ( $D$ ) are presented below in Figure 25.

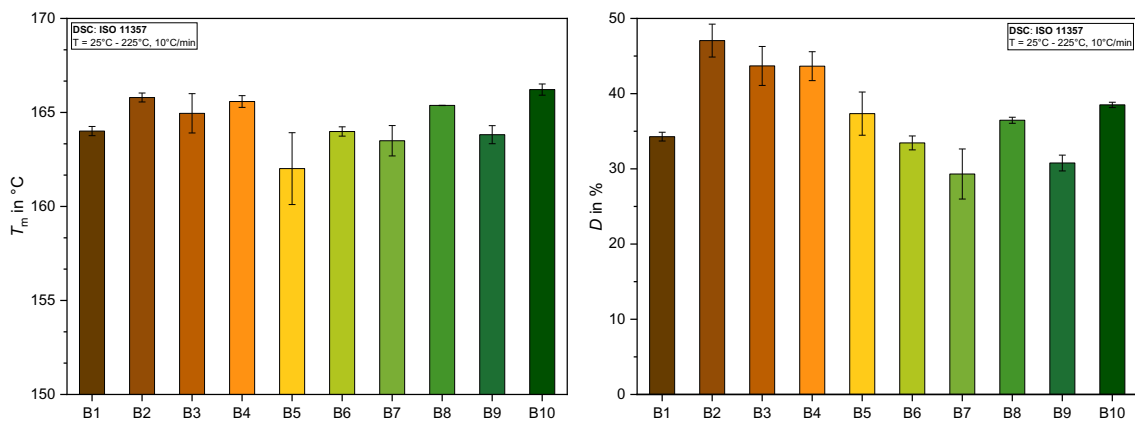


Figure 25: Left: melting temperature  $T_m$ , right: crystallinity  $D$ .

The  $T_m$  tends to be lower for filled (B1, B9) than for unfilled materials (J. Schöne et al. 2012). However,  $T_m$  is not significantly affected by the filler content. More striking are results regarding  $D$ . As for other tests that were performed, B1, B7 and B9 show similarities. It seems that with increasing filler content,  $D$  decreases. For B1 and B9 a significant lower  $D$  (~31 %) compared to B2 (47 %) occurred. However, the reason why the same phenomenon occurs for B7 cannot be related to the filler content.

#### 4.4 Thermogravimetric analysis

Representative TGA curves of all batches are given in Figure 26. At a temperature of 430 °C to 440 °C all batches show the most pronounced peak, indicating PP decomposition with around 70 % of weight loss (Ehrenstein et al. 2012). But the first decomposition step occurs for B2 and B6 at 280 °C. This may be an effect of polyvinylchloride (PVC) impurities (Mettler-Toledo 2022). Another decomposition step is reached at around 600 °C. At this temperature the residual weight decreases again about 5 % except for B1 and B9 where it is just 1 %. This small step at around 600 °C refers to CaCO<sub>3</sub> decomposition. It decomposes in a nitrogen atmosphere, talc in contrast, does not show any mass loss (Ehrenstein et al. 2012). As a result of that, B1 excels with a filler content of 26 % followed by B9 with around 18 %. Remaining batches exhibit a filler content in a range of 8 - 11 %. High filler content might be the reason for deviations of B1 and B9 in several testing procedures (DSC, density,  $\sigma_V$ ,  $k_z$ ), however, not an indication why B7 also deviates like B1 and B9 in the same test methods. The residual weight of all samples at 720 °C, still more than 8 %, indicates additional non-decomposed inorganic fillers.

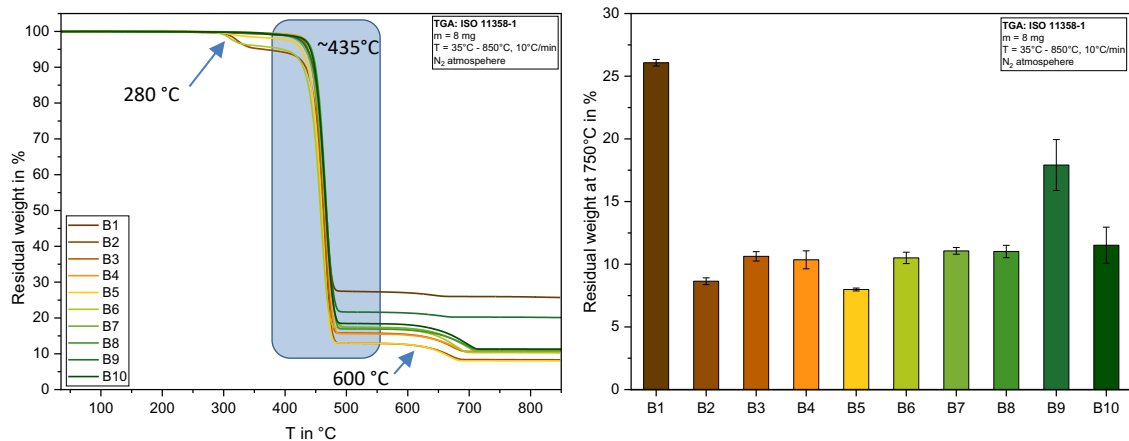


Figure 26: Left: TGA curves (residual weight over temperature), right: residual weight in % of each batch at 750 °C.

Big differences considering residual weight after the decomposition steps were discovered. Since no material data was included with the batch supplies, the partially high filler content was surprising.



## 4.5 Dynamic mechanical analysis

Graphs below show results of DMA measurements for  $E'$  and  $E''$  of each batch (see Figure 27). Around 0 °C all batches show a storage modulus in a range from 3500 MPa to 4500 MPa and drop to ~ 1000 MPa at 75 °C. The steeper slope of the curves around 0 °C indicates  $T_g$  which is clearly visible at a temperature between -0,5 °C and 3,5 °C (blue framed). Small fluctuation of  $T_g$  from - 5°C to 3.5°C may occur due to bulky side chains or hindrance of main chain movement (Ehrenstein 2011). For B6  $E'$  is at a significantly lower level in the temperature range from - 75 °C to 0 °C compared to other batches.

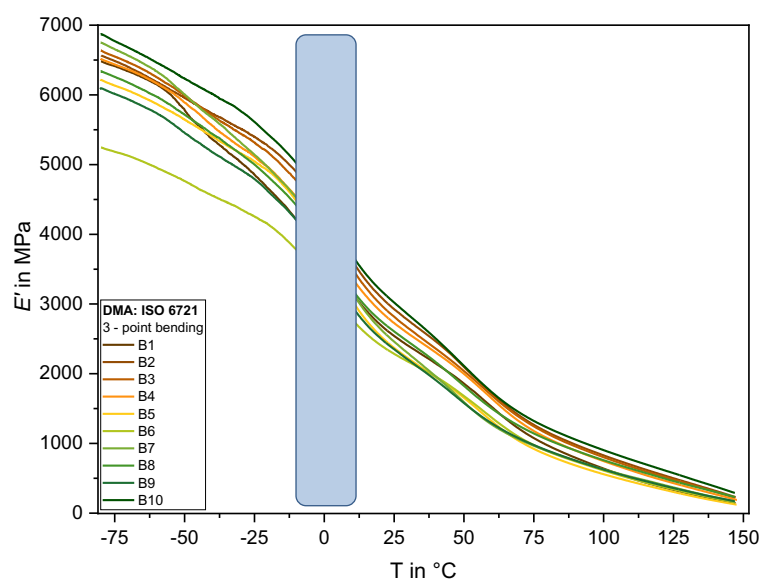


Figure 27: Storage modulus  $E'$  over temperature  $T$  for B1 – 10.

If  $E''$  is examined more closely, it is noticeable that B1, B7 and B9 clearly exhibit a second peak at a temperature of about - 50 °C. For B4 and B8, this peak is also present, but not as pronounced. Remaining batches do not show any conspicuous peak in this area at all. In order to compare this more accurately, results for loss modulus are shown separately in Figure 28.

In theory, due to high content of mineral reinforcement, in this case talc, B1 and B9 should have a comparably high  $E'$  and  $E''$  for PP (Florian J. Arbeiter et al. 2016). Nevertheless, it seems that talc has no significant influence on  $E'$  or  $E''$  for recycled PP filled with talc.

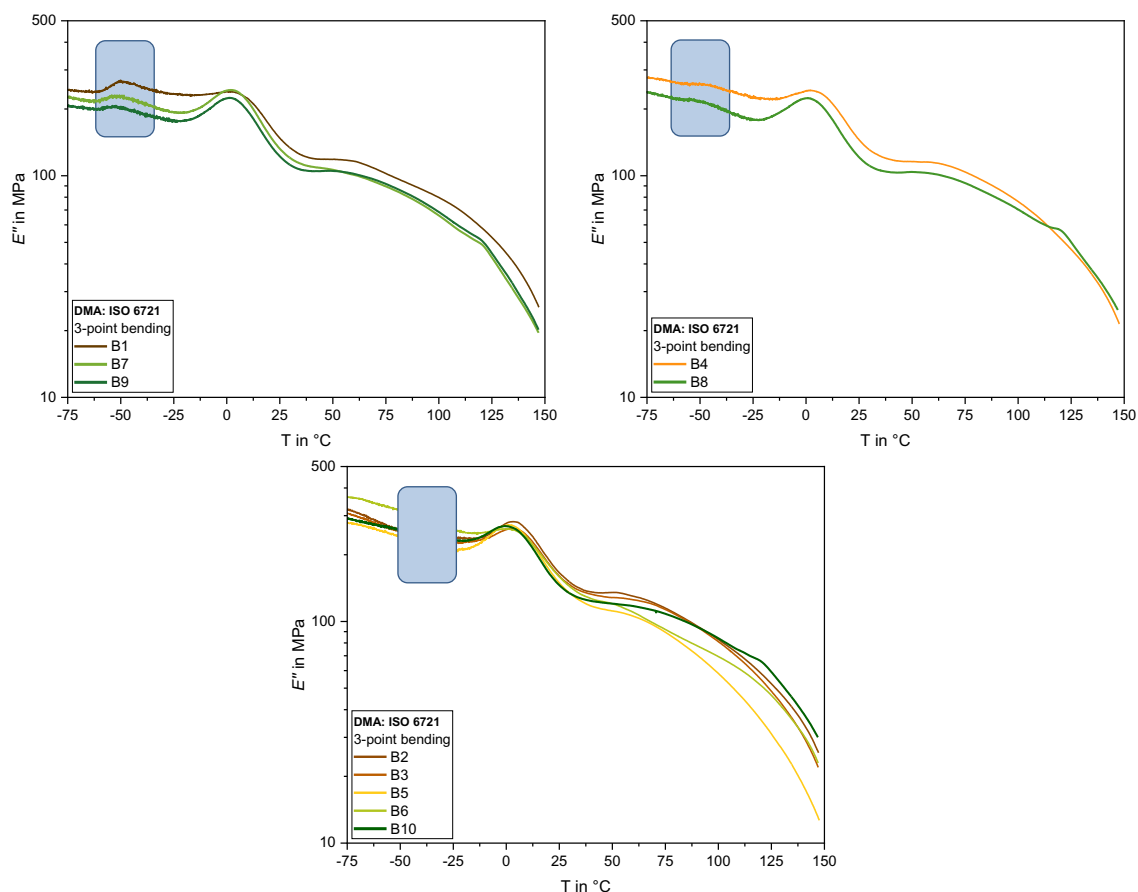


Figure 28: Loss modulus  $E''$  for B1-10, pronounced peak at  $-50^{\circ}\text{C}$  (top left), small peak at  $-50^{\circ}\text{C}$  (top right), no peak at  $-50^{\circ}\text{C}$  (bottom center).

The additional peak at  $-50^{\circ}\text{C}$  might indicate a so called  $\beta$  – transition ( $T_n$ , secondary transition), a softening of  $-\text{CH}_2-$  chain segments, for B1, B7 and B9. Thus, these batches may have a higher degree of branching. The beginning of rearrangement of molecular segments or of side groups may take place (Ehrenstein 2011). However, if this assumption is compared with the rheological measurements and the concept of the crossover point, this cannot be confirmed.

#### 4.6 Fourier Transform Infrared Spectroscopy

As an alternative technique to quantify the different compositions of polymer batches in terms of the different vibrational modes of these units FTIR-ATR spectroscopy was used. In Figure 29 a representative spectrum for each batch is given.

For the PP batch variation under investigation, characteristic  $\text{CH}_2$  and  $\text{CH}_3$  bands were determined in the range of  $2955\text{ cm}^{-1}$  to  $2835\text{ cm}^{-1}$ . Looking deeper into the spectra, it is observable that the most intense band for every batch is localized at  $2918\text{ cm}^{-1}$  in form of

an asymmetric stretching vibration of the material's CH<sub>2</sub> molecules. Furthermore, for all batches a peak with high intensity occurs at 1376 cm<sup>-1</sup> which is related to either a symmetric bending vibration of CH<sub>3</sub>, a bending of CH molecules, a wagging of CH<sub>2</sub> molecules or a stretching of CC-backbone, typical for PP. (Andreassen 1999).

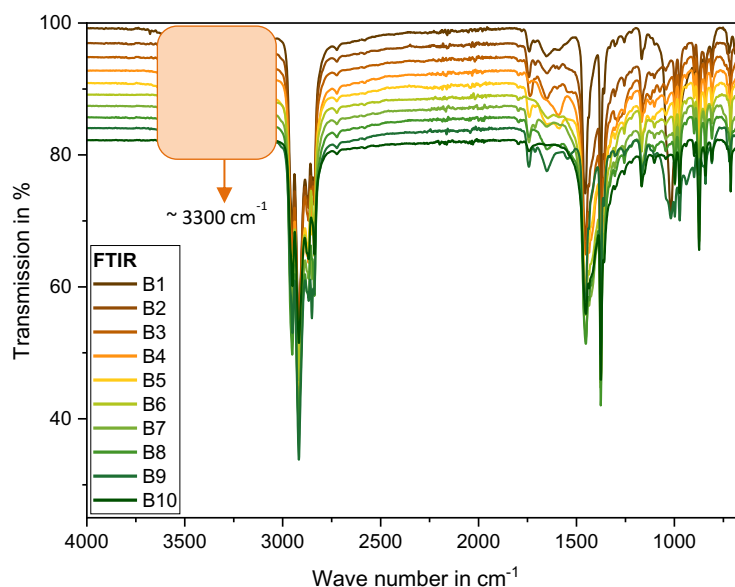


Figure 29: Representative FTIR spectra for B1-B10.

All batches, with the exception of B10, have a broad band in the range from 3600 cm<sup>-1</sup> to 3050 cm<sup>-1</sup>. This is reducible to OH vibrations from degradation or impurities. In liquid or solid state, alcohols and phenols, whose OH group is not sterically shielded, have a very broad absorption band in that region, with maximum being around 3300 cm<sup>-1</sup> (Günzler 2003).

Important to point out is the pronounced band at a wavenumber of 1018 cm<sup>-1</sup> for B1 and B9. For better comparability, B1 and B9 are depicted in Figure 30 together with B2. This band (blue framed) is due to high talc content in those two batches. By means of TGA, it was found that the recyclates contain fillers. Results from FTIR measurements support the assumption that these fillers are talc and CaCO<sub>3</sub>, respectively. Further, B1 is the only batch that has a tiny band at 3675 cm<sup>-1</sup> (blue framed, Figure 30) which corresponds also to the high content of talc. Compared to the other batches B1 and B9 may show a high talc content, but in contrast to the rest, B1 and B9 do not exhibit a band at 712 cm<sup>-1</sup> (green framed), indicating presence of CaCO<sub>3</sub>. This is also in accordance with TGA results, where

B1 and B9 do not show any pronounced decomposition step for  $\text{CaCO}_3$  at 600 °C where all other batches do.

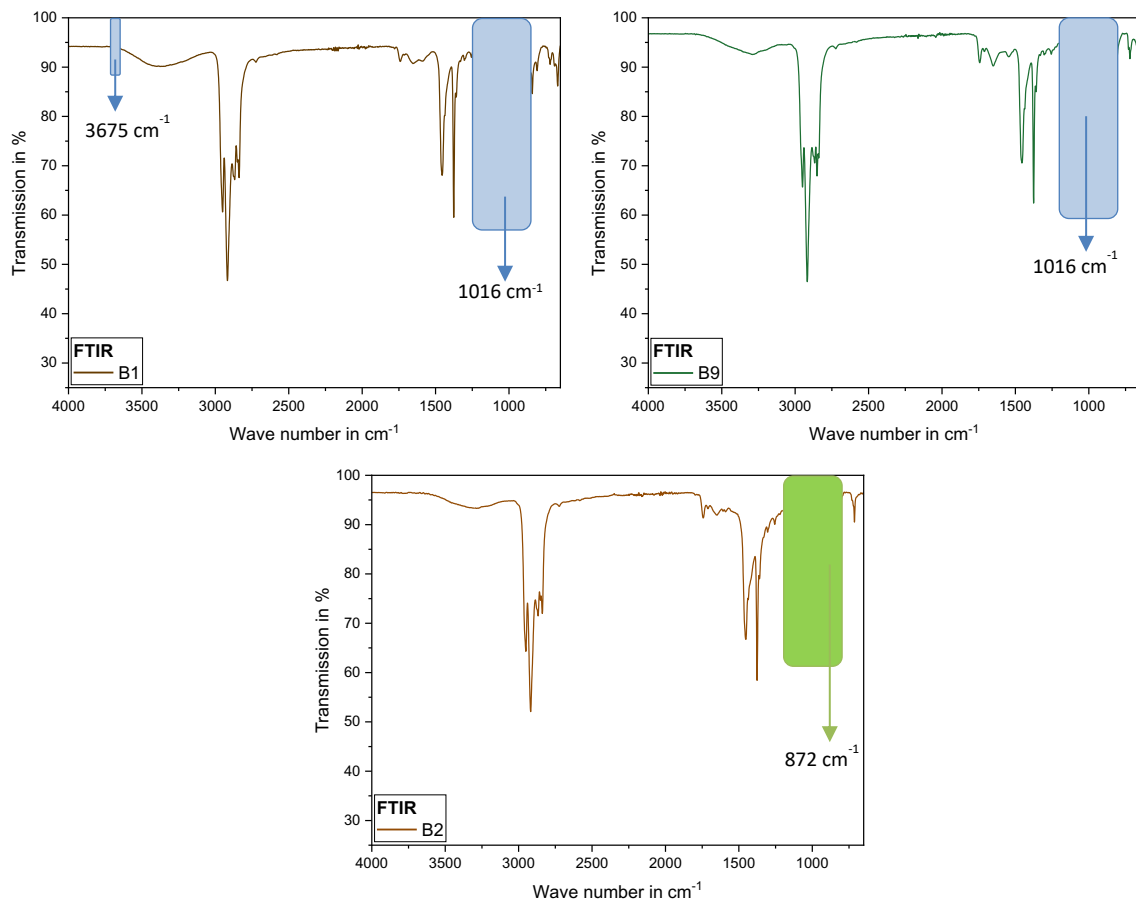


Figure 30: Comparison of B1, B9 and B2 considering talc band (blue framed), respectively  $\text{CaCO}_3$  band (green framed).

#### 4.7 Tensile test

In Figure 31 representative stress-strain curves ( $\sigma$ - $\epsilon$ ) for each batch are depicted. Batches show variations considering  $\sigma_y$ ,  $E$  and high deviations for  $\sigma_b$ . Results for those material properties are given in Figure 33. The lowest value for  $E$  occurs for B5 with 1466 MPa followed by B7 with 1667 MPa. Highest value was recorded for B10 with 2020 MPa, respectively by B2 with 1940 MPa. Other batches show values between 1730 MPa and 1940 MPa. Scattering is higher for B1 to B5. Difference of  $E$  in scatter of B1-B5 compared to B6-B10 may be explained by several months been between the two series of measurements. The applied makro system was disassembled and reassembled in between. Looking at the results for  $\sigma_y$ , value range is from 22 MPa (B1) to 31 MPa (B2). Again, B1, B7 and B9 show similar values around 22 MPa whereas the rest of the batches have a

significantly higher  $\sigma_y$  with  $\sim 27$  MPa. This phenomenon can be attributed to high filler content, which reduces  $\sigma_y$  (J. Schöne et al. 2012). This lowering of  $\sigma_y$  can be connected to the debonding of the particles from the polypropylene matrix (W.C.J Zuiderduin et al. 2003). Results for  $\sigma_y$  results show smaller standard deviation in contrast to  $E$ .

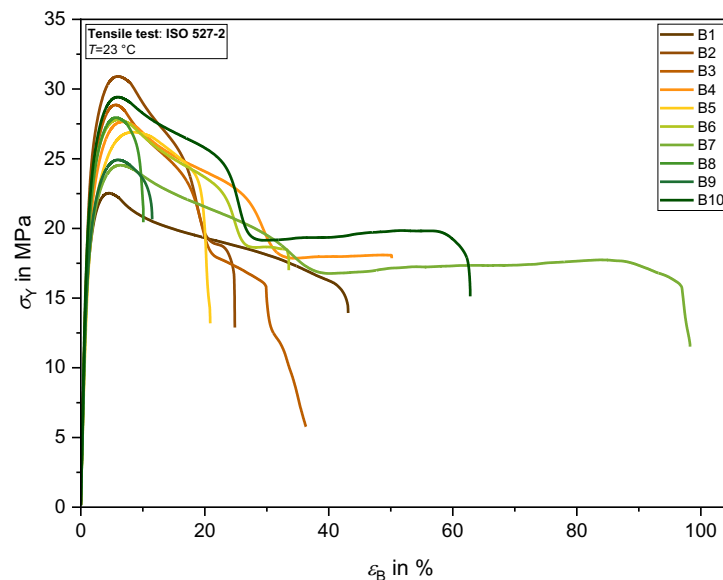


Figure 31: Representative stress-strain ( $\sigma$ - $\varepsilon$ ) graphs for B1-B10.

Considering results of  $\varepsilon_b$ , B7 excels with 100 %, but also shows the most pronounced standard deviation of results.

All specimens were injection molded with the same parameters (as it should be the same material). But the phenomenon of blowholes just occurred for B3, B4, B8 and B9 (see ). During the holding pressure phase, quality of molded part, dimensional accuracy, etc. are influenced by the pressure profile. Blowholes are caused, for example, by insufficient adjustment of the melt and/or mold temperature (Steinko 2008).



Figure 32: Blowholes of B3, B4, B8 and B9.

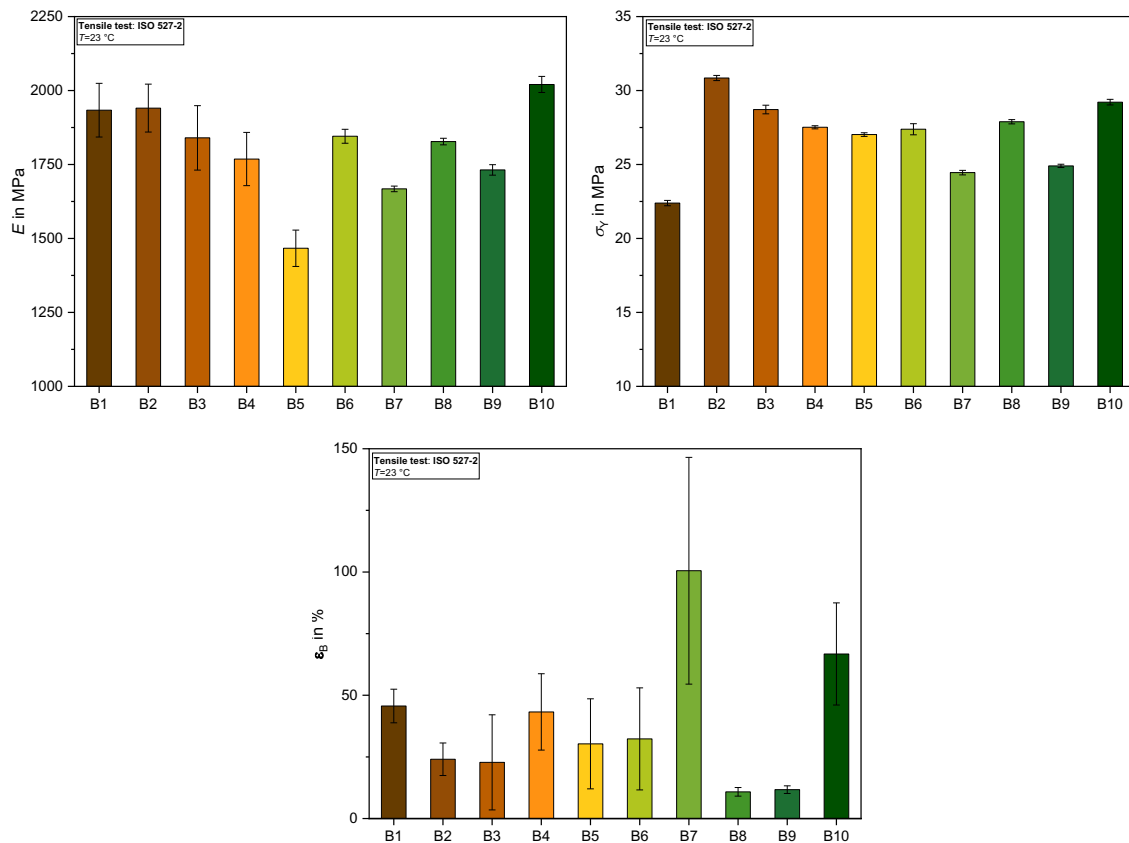


Figure 33: Young's modulus  $E$  (top left), yield stress  $\sigma_y$  (top right), strain at break  $\epsilon_B$  (bottom center) for B1-B10.

### 4.8 Charpy impact test

Charpy notched and unnotched impact test produced a complete brittle fracture for each batch. Measured specimens for B2 are schematically shown in Figure 34. Results of notched and unnotched impact strength as well as notch sensitivity are given in Figure 35.

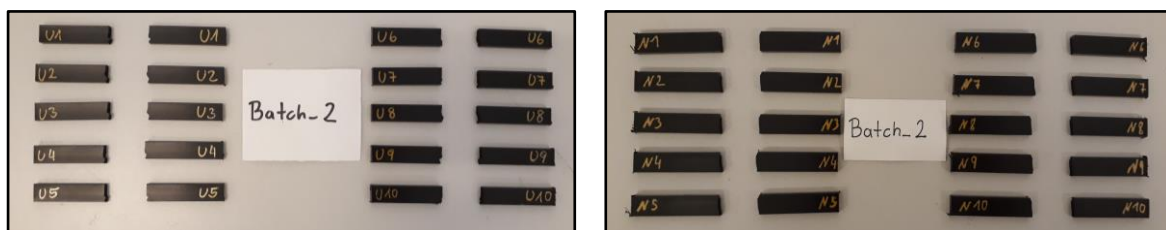


Figure 34: Charpy impact test, B2 tested specimens, left: unnotched, right: notched.

Results for Charpy notched and unnotched impact strength show high variations within the investigated batches (see Figure 35). Lowest value occurs for B2 with 47 kJ/m<sup>2</sup> followed by B9, B6 and B1. Remarkably high is the result for B7 with an unnotched impact strength of

111 kJ/m<sup>2</sup>. Remaining batches (B3, B4, B5, B8, B10) are in a middle range from 67 - 87 kJ/m<sup>2</sup>.

Notched impact strength showed a similar trend in values. Again, with 3 kJ/m<sup>2</sup> B2 has the lowest (followed by B6 and B9) and B7 the highest value. For B3, B4, B5, B8 and B10 results are in a same range, from 3.6 – 4.6 kJ/m<sup>2</sup>. With the exception of B1 and B4, all batches have the same qualitative values for  $a_{cN}$  and  $a_{cU}$ . For unnotched impact strength it settled among the three lowest, for notched impact strength it ranks the second highest.

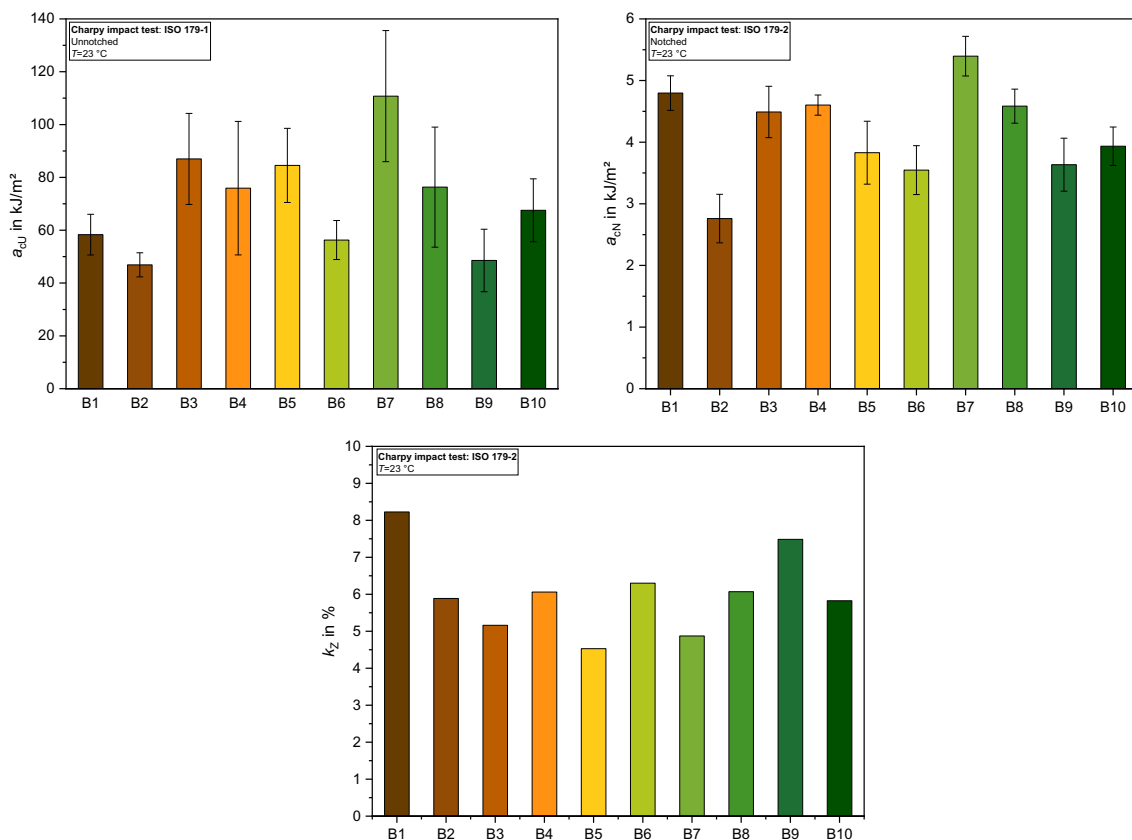
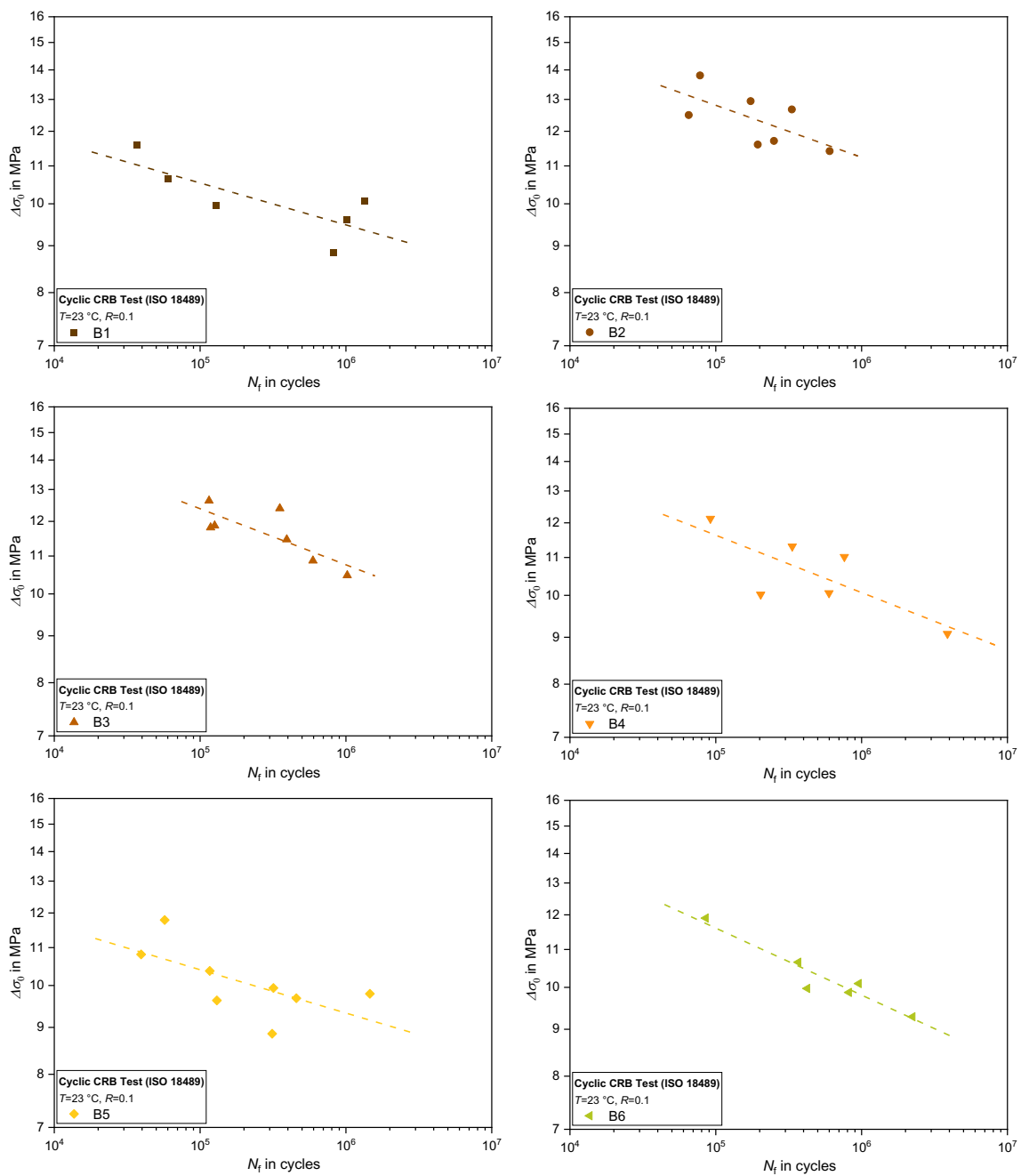


Figure 35: Unnotched impact strength  $a_{cU}$  (top left), notched impact strength  $a_{cN}$  (top right), notch sensitivity  $k_z$  (bottom center) for B1-B10

Out of unnotched and notched impact strength, notch sensitivity was calculated. With more than 8 % B1 has the highest value for notch sensitivity directly followed by B9 with 7.5 %. This can be attributed to the elevated talc content, which has a negative effect on impact strength (Bakar et al. 2007; Lapcik et al. 2009). In the middle range are B2, B4, B6, B8 and 10 with a notch sensitivity of about 6 %. Last in the row is B5 with 4.5 %, followed by B7 (4.8 %) and B3 (5.1 %).

### 4.9 Lifetime under cyclic load via CRB test

Failure under cyclic load is considered a time-dependent phenomenon in viscoelastic thermoplastics. It is characterized by means of CRB test which is widely accepted as testing method for long-term structural applications. To give a clear representation of the batches tested via cyclic CRB test, results are shown for each batch individually (Figure 36). In following diagrams  $\Delta\sigma_0$  is plotted against  $N_f$  and the scale is the same for all batches.





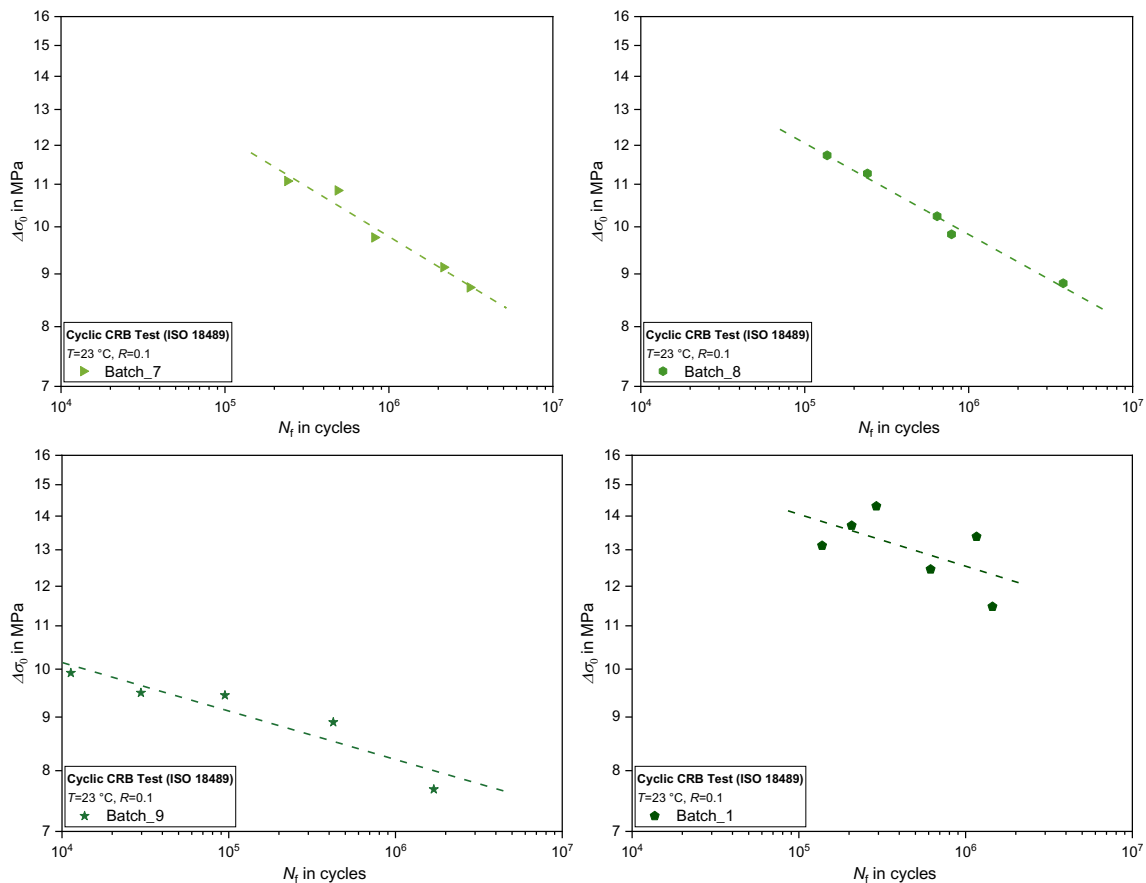


Figure 36: Failure cycle numbers  $N_f$  as a function of the applied stress range  $\Delta\sigma_0$  for B1-B10 (ISO 18489).

At least five specimens were tested for each material. Due to the high scatter, more measurements were performed for some batches. Even at first glance, it is obvious that there are significant differences between batches in terms of long-term behavior. One reason for the rather different results in the cyclic CRB test is the filler content.

In the cyclic CRB test, B10 performs best by far, followed by B2. The worst result among all batches was clearly reached of B9, followed by B5 and B1. For better comparison, results of these four batches are shown in one diagram (Figure 37). With more than 20 % talc content B9 and B1 show a significantly lower service life under cyclic loading compared to the other batches. As stated in literature, a high talc content leads to a higher susceptibility to cracks and fractures (Florian J. Arbeiter et al. 2016; Grellmann 2011). It reduces the material's ability to undergo plastic deformation (J. Schöne et al. 2012). However, B5 has the lowest filler content but shows low performance in cyclic CRB test and also  $E$  was lowest for B5. Thus, there is a certain amount of filler that improves long-term behavior, whereas

too much filler reduces it. Therefore, it is important how much filler is added to a recycle to achieve requested material properties.

If the results of MFR are referred to, it can be stated that those with a comparably low MFR provide good results in the cyclic CRB test, i.e. long-term behavior. However, for this assumption the filler content must be taken into consideration because for B1, which also has a low MFR, the lifetime under cyclic load decreases.

Results for the remaining six batches are located between B1 and B2 (blue framed area). Additional in Figure 37 results for B7 are included to draw attention to the deviating slope of the linear regression. Apart from B7, also B6 and B8 show a steeper slope of linear fits, with only a small scattering of results.

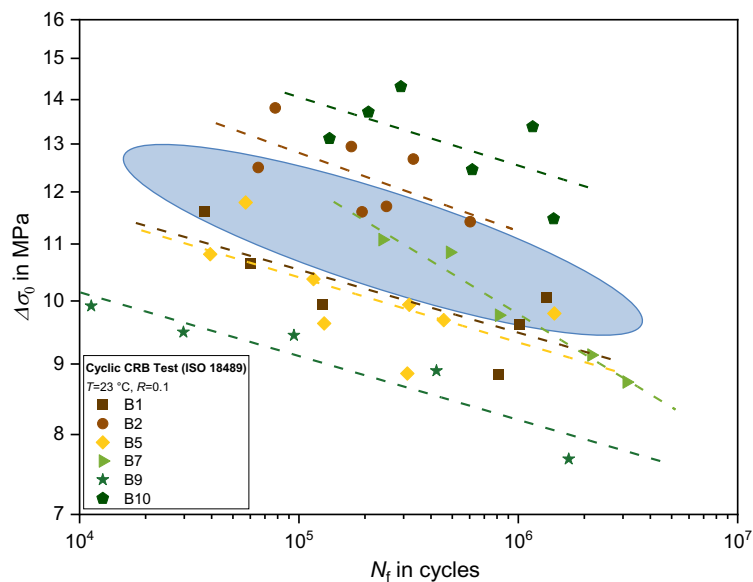


Figure 37: Failure cycle numbers  $N_f$  as a function of the applied stress range  $\Delta\sigma_0$ , comparison best (B2, B10) and worst (B1, B5, B9) performance, B7 with steeper slope.

Except for B6, B7, B8 and B9, results of the cyclic CRB test scatter strongly. In particular, for B1, B2, B3, B4, B5, and B10, it depends on which measurements are considered outliers and, to a large extent, through which data points a regression is drawn. After optical measurements (light microscopy, SEM), however, no obvious effect was observed which would explain outlining of some data points. It is either on a much higher or lower level or has a completely different slope. This scenario was run schematically with results for B5 and is shown in Figure 38. At a stress level of 10 MPa (mean value between lowest and highest

load) a reference line was drawn to reflect at which cycle number B5 would have failed depending on the regressions position.

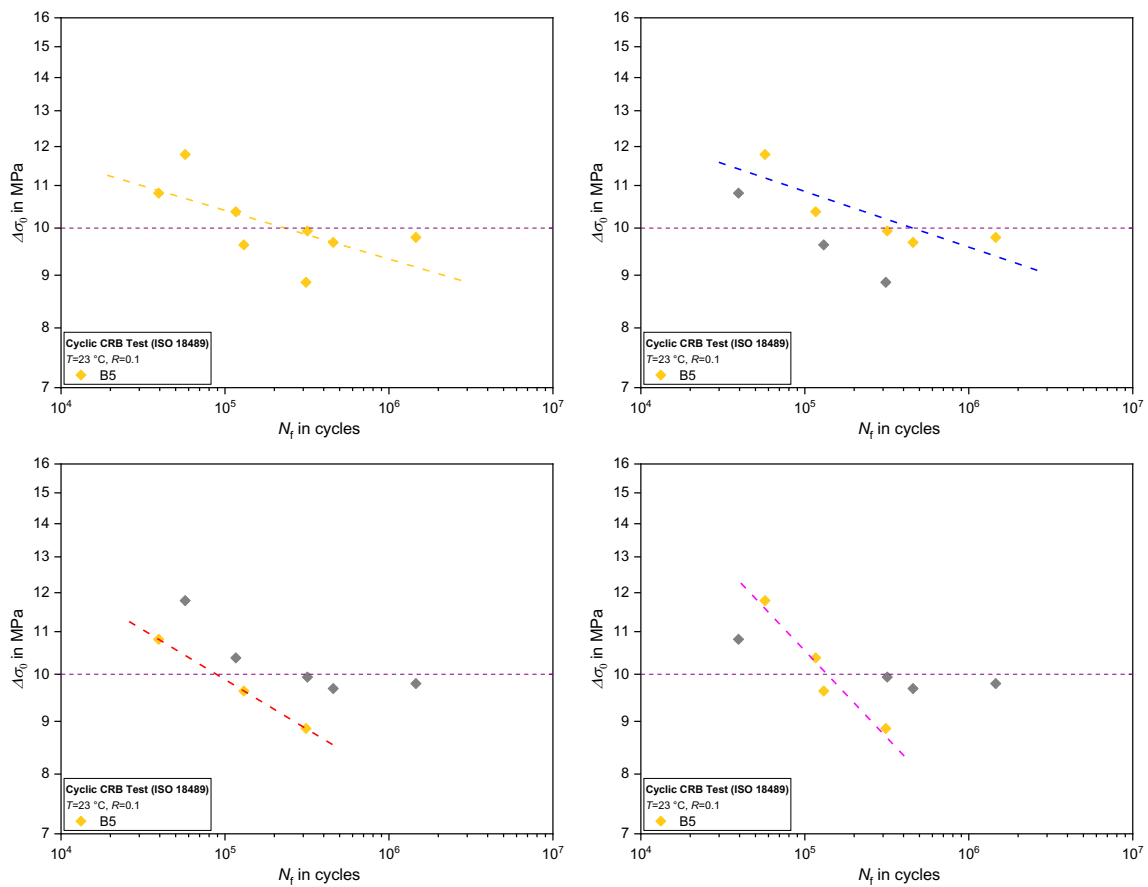


Figure 38: Failure cycle numbers  $N_f$  as a function of the applied stress range  $\Delta\sigma_0$ , different possibilities of regression for B5.

Predicted  $N_f$  for different possibilities of regression for B5 is given in Table 6. For the originally drawn regression (yellow) with all results gained for B5, failure at 10 MPa would occur after 231150 cycles. When taking the most conservative results (red), failure would occur already at 86840 cycles, less than the half. Considering the most unconservative test result for B5 (blue),  $N_f$  for  $\Delta\sigma_0 = 10$  MPa would appear after 465125 cycles – more than five times longer than the conservative result and twice as long as the result regarding all data. Results are also strongly dependent on which data points are traded as outliers. In case of the pink regression, the slope of the curve is completely different, which influences the prediction of failure ( $N_f$  at 135600 cycles). If these different possibilities are now compared with the approach of the standard for PCR - PP with regard to cyclic CRB test (ONR CEN/TS 14541-2), it becomes obvious how inadmissible the application of this standard is.

After optical analysis of the fracture surface, no obvious defects were found that would explain any outliers. Due to this, in case of recyclates a regression should be drawn by considering all data points, since it is not possible to determine actual outliers.

Table 6: Prediction of cycles until failure  $N_f$  at 10 MPa for different regressions for B5.

Regression	$N_f$ at 10 MPa in cycles
Yellow (all data)	231.150
Red (conservative)	86.840
Blue (unconservative)	465.125
Pink (slope)	135.600

Analysis of SEM images led to further insight of the batches long-term performance. In Figure 39 representative SEM images of a high filled batch (B1) and a low filled batch (B5) are shown at 2000 x magnification. For comparison, only the SEM images taken near the pre-inserted notch were considered. It is clearly visible that B1 has a much higher content of plate-shaped talc impurities than B5 and that the fracture surface is different. In case of B5 the fracture surface is much smoother, whereas for B1, formation and breakdown of fine fibrils can be seen near the pre-notch, with talc plates in between.

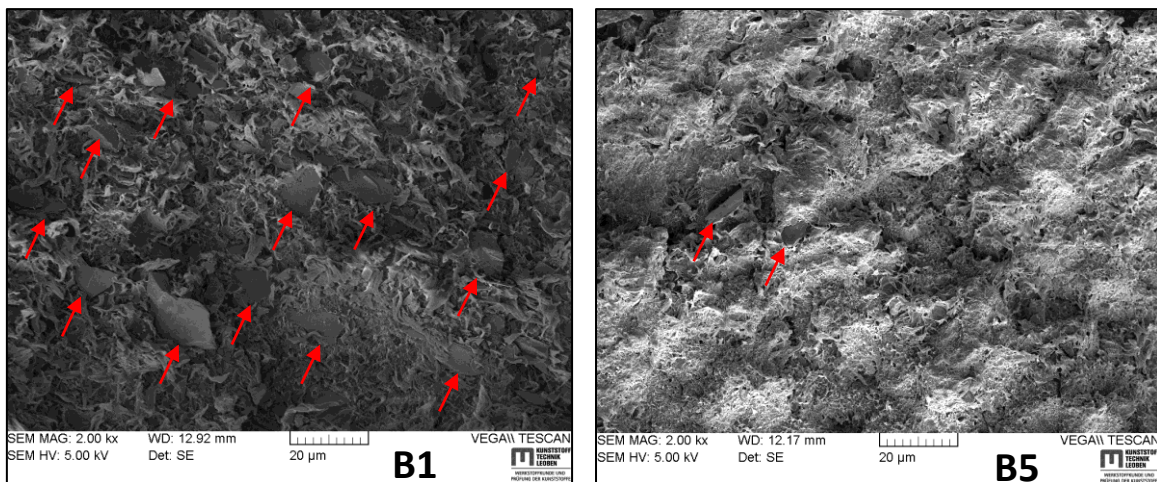


Figure 39: SEM analysis for B1 (left) and B5 (right).

In order to estimate how virgin material blended with recyclate behaves in CRB test, the best performing batch in CRB test (B10) and one of the worst batches (B5) were mixed in a ratio of 75/25 with vPP (virgin/recyclate). Results are depicted in Figure 40.

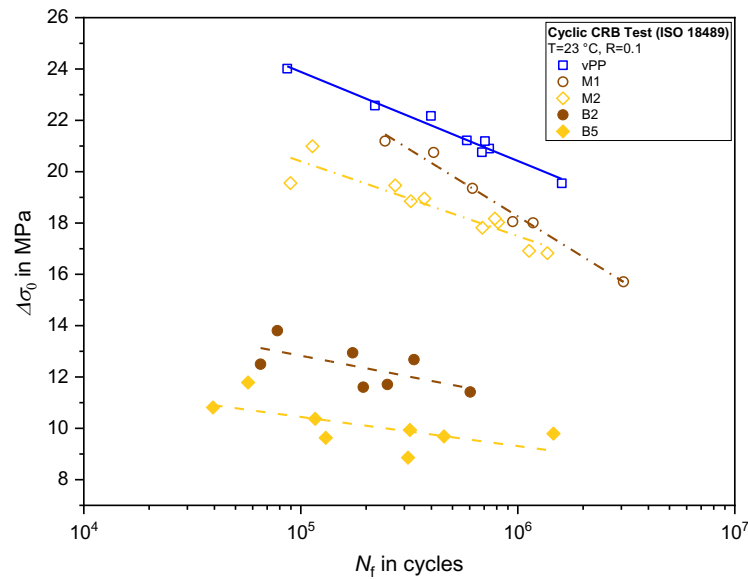


Figure 40: Failure cycle numbers  $N_f$  as a function of the applied stress range  $\Delta\sigma_0$ , vPP and blends M1 and M2.

The compact blue line represents CRB test results for vPP. The dashed lines show long-time behavior of pure recyclate batches (B5, B10) and dash-dotted lines visualize results of material mixtures M1 and M2. For vPP a clear linear dependence of the failure curve can be observed. Increasing the load  $\Delta\sigma$ , leads to a decrease of  $N_f$  in a double logarithmic diagram.

As expected vPP shows a better long-term behavior compared to the pure recyclates. However, blending pure recyclate batches with vPP does not compensate batch variations as it can be seen from the data shown in Figure 40. Nevertheless, the trend stays the same, a "good" batch mixed with virgin material performs better than a "bad" batch in CRB test does. So, blending pure recyclate batches with vPP does not compensate batch variations. If blending PCR - PP with vPP would compensate batch variation completely, curves would lie on one line, which is not the case. But Figure 40 shows that mixing batches with virgin material reduces high deviation of datapoints. Single points are all significantly closer to the linear regression applied than in case of the pure recyclate batches.

The failure curves of vPP and the blend with B5 are almost parallel. Comparing virgin material and blend with B2, a steeper slope for the blend is visible. This can be an indication for different failure mechanisms of the materials. But on fracture surfaces no anomalies, which may be a reason for lower or higher  $N_f$  were observed. However, it can be seen that

the curves of the two blends approach each other at high  $N_f$ , since the slope of B2 is steeper. But for more information about that phenomenon, the determination of additional points is necessary.

Preliminary results show that analyzing lifetime of a recyclate (a material with significantly lower performance) as well as a blend of virgin material and recyclate by means of CRB test is possible. Nevertheless, lifetime of virgin material is drastically reduced due to recyclate content (Hinczica et al. 2022).

## 5 SUMMERY AND CONCLUSION

The versatility of plastics in numerous applications has led to rapid growth in global plastics production. Especially for disposable products such as packaging or bottles as well as for structural applications. As growing production is inevitably accompanied by increasing amounts of plastic waste, serious challenges arise in terms of disposal. A functioning circular economy would be beneficial, where plastic waste is treated as a valuable secondary raw material where much more recycled material finds its way back into useful applications. Additionally, landfilling should be prevented as far as possible in view of environmental protection and global warming. In order to find new ways for sustainable use of recycled polymers in structural long-term applications such as building or construction sector, fundamental studies on modification of material properties of recyclates or batch variations are needed.

Buying one and the same recyclate over a period of time does not ensure getting a material with equal, or even similar properties. This thesis demonstrates rather well, how big the problem of batch variations truly is. By performing many different testing procedures, high variation in several properties of ten recycled batches of PP were found. For example: Comparing MFR value of two batches delivered directly one after the other (B1, August 2021 and B2, September 2021), the MFR value has doubled. This is mainly due to insufficient waste sorting in the recycling process. Further, the amount of inorganic ingredients fluctuates significantly over time. Application of fillers in recycled material is a common method to improve mechanical properties in terms of stiffness, strength and impact resistance. Presence of talc and  $\text{CaCO}_3$ , respectively chalk in batches were determined by means of TGA and FTIR. From DSC experiments it was shown that the filler content had small influence on  $T_m$  but on  $D$  of the PP phase. For filled batches  $T_m$  tends to be lower than for unfilled batches and  $D$  seems to decrease with increasing filler content. Depending on filler content, huge differences in terms of mechanical and long-term properties were discovered.

Up to now, no statements can be made about seasonal fluctuations because there is little to no research on this. So, it cannot be said that high filler content in B1 and B9 is related to the fact that these two batches were delivered in midsummer (July and August) because

there is too little information about the recyclates delivered. The manufacturer did not even know about any filler content in the material ordered. Keyword “little information about recyclates” can be undergirded with the evaluation of TDS. The study of Hans-Josef Endres and Madina Shamsuyeva, 2020 demonstrates well, which standard test procedures PP and recyclates out of PP undergo at suppliers (see Figure 7, chapter 2.2.2). Most performed standardized measurements which deliver comprehensible material properties are MFR, Charpy impact tests and density. But according to this study, out of 51 TDS from eleven companies there is no viable statement about recyclate content in materials. There was also insufficient information about tensile properties, thermal oxidation stability or  $T_m$ . For manufacturers this means time and money consuming material testing before an arrived batch can be used for further processing, although the same material was ordered. Regarding this thesis, all investigated batches are within the acceptable MFR range supplier and manufacturer agreed on. Results for mechanical properties and lifetime under cyclic load are not similar or even comparable. High filled batches (B1, B9) show nearly double the value for  $k_z$  compared to the least filled batch (B5). Tensile test results should be taken in consideration with caution. With filler content  $\sigma_y$  was lowered which can be connected to the debonding of the particles from the PP matrix. By naked eye no defects for injection molded specimens were visible but four materials had blowholes in produced multipurpose specimens. Each batch was injection molded using the same parameters (see chapter 3.1). With just ten batches of an assumed same material it is already evident that injection molding process would have had to be adapted individually for each batch in order to guarantee flawless test specimens.

Further, making viable statements about long-term behavior of batches by means of cyclic CRB test turned out to be difficult. Results for most batches showed high scattering which makes applicability of an already existing standard (ONR CEN/TS 14541-2) for PP recyclates nearly impossible. By measuring two data points of a recyclate material, connecting them and comparing that with results of a certain reference material regarding long-time performance does not give representative statements. For batches under investigation cyclic CRB tests were performed at test loads from  $\Delta\sigma_{\min} = 8.5$  MPa to  $\Delta\sigma_{\max} = 15$  MPa, because no valid results could be generated in the cyclic CRB test for the load intervals



specified in the standard (13 – 16 MPa). So, using just this standard to determine whether a recyclate is good or bad would be insufficient and somehow negligent. Deviations are too high, for that principle to work properly (see Figure 38).

It was also proven, that lifetime of virgin material blended with 25 % PCR is reduced drastically (see Figure 40). The extent to which long-term properties of virgin materials blended with recyclate deteriorate depends on recyclate quality. Good recyclate (constant feedstock, well sorted and processed) reduces proper long-term performance less than a bad recyclate (Hinczica et al. 2022).

Goal of industry is finding fast methods to gain information about materials (recyclates) regarding long-term performance. Results of some standardized testing methods, that can be carried out quickly showed slightly correlations with lifetime under cyclic load. But no distinct correlation was found. This underlines the great importance of material characterization with specific focus on lifetime under cyclic load. A combination of results from MFR, Charpy impact strength, TGA, FTIR and tensile properties ( $\sigma_y$ ) can give an indication of long-term behavior. However, it cannot replace a cyclic CRB test which provides representative results on long-term behavior of a material. In any case, corresponding standards should be adjusted.

At this stage, further studies are highly recommended to clarify the influence of inorganic ingredients (e.g. fillers or other solid impurities), influence of blending levels and the influence of different reprocessing steps during recycling. The range of permissible parameters defined between supplier and manufacturer should be reduced to guarantee stable processability. To successfully fulfill issues of the European Circular Economy Action Plan, more information on recyclate in all aspects (feedstock area, storage time, season of collection, etc.) would be urgently needed to increase the use of recyclates in various applications for a functioning circular economy in a world dominated by plastics.

## 6 PUBLICATION BIBLIOGRAPHY

Ammar O; Bouaziz Y; Haddar N; Mnif N (2017a): Talc as Reinforcing Filler in PolypropyleneCompounds: Effect on Morphology andMechanical Properties. In *Polymer Sciences* 3 (2), p. 0. DOI: 10.4172/2471-9935.100023.

Ammar O; Bouaziz Y; Haddar N; Mnif N (2017b): Talc as Reinforcing Filler in PolypropyleneCompounds: Effect on Morphology andMechanical Properties. In *Polymer Sciences* 3 (2), p. 0. DOI: 10.4172/2471-9935.100023.

Andreassen, Erik (1999): Infrared and Raman spectroscopy of polypropylene. In : *Polypropylene*: Springer, Dordrecht, pp. 320–328. Available online at [https://link.springer.com/chapter/10.1007/978-94-011-4421-6\\_46](https://link.springer.com/chapter/10.1007/978-94-011-4421-6_46).

Anke Herold; Vanessa Cook; Yifaat Baron; Martin Cames; Sabine Gores; Jakob GRAICHEN et al. (2023): EU Environment and Climate Change Policies. State of Paly, current and future challenges. Anke HEROLD, Vanessa COOK, Yifaat BARON, Martin CAMES, Sabine GORES, Jakob, checked on 6/28/2023.

Avani Group of Industries (2020): Talc in Plastics & Polymers - Avani Group of Industries. Available online at <https://avanitalc.com/applications/talc-plastics-polymers/>, updated on 6/20/2020+00:00, checked on 4/3/2023.047Z.

Bakar, M. B. Abu; Leong, Y. W.; Ariffin, A.; Ishak, Z. A. Mohd. (2007): Mechanical, flow, and morphological properties of talc- and kaolin-filled polypropylene hybrid composites. In *Journal of Applied Polymer Science* 104 (1), pp. 434–441. DOI: 10.1002/app.25535.

Bonten, Christian (2016): *Kunststofftechnik. Einführung und Grundlagen. 2., aktualisierte Auflage.* München: Hanser.

Cosmacon (2022): Talkum - Talk - Steatit - Magnesiumsilikathydrat - Cosmacon. Available online at <https://www.cosmacon.de/talkum/>, updated on 10/23/2022+00:00, checked on 4/3/2023.791Z.

ISO 179-2: DIN EN ISO 179-2, checked on 2020-09.

DIN EN ISO 3219-2, 2021: DIN EN ISO 3219-2:2021-08, Rheologie\_ - Teil\_2: Allgemeine Grundlagen der Rotations- und Oszillationsrheometrie (ISO\_3219-2:2021); Deutsche Fassung EN\_ISO\_3219-2:2021.

Domininghaus, Hans; Elsner, Peter; Eyerer, Peter; Hirth, Thomas (2012): Kunststoffe. Berlin, Heidelberg: Springer Berlin Heidelberg.

Ehrenstein, G.; Riedel, G.; Trawiel, P. (2003): Praxis der Thermischen Analyse von Kunststoffen von Gottfried Wilhelm Ehrenstein | ISBN 978-3-446-22340-0 | Fachbuch online kaufen - Lehmanns.de. Edited by Hanser. München. Available online at <https://www.lehmanns.de/shop/naturwissenschaften/5406929-9783446223400-praxis-der-thermischen-analyse-von-kunststoffen>, updated on 4/6/2023.000Z, checked on 4/6/2023.445Z.

Ehrenstein, Gottfried W. (2011): Polymer-Werkstoffe. Struktur - Eigenschaften - Anwendung. 3. Auflage. München: Hanser. Available online at <http://www.hanser-elibrary.com/doi/book/10.3139/9783446429673>.

Ehrenstein, Gottfried W.; Riedel, Gabriela; Trawiel, Pia (2012): Thermal Analysis of Plastics. Theory and Practice: Carl Hanser Verlag GmbH Co KG.

Feng, Yuding; Jin, Xiaorong; Hay, James N. (1998): Evaluation of Multiple Melting Peaks of Propylene-Ethylene Copolymers. In *Polym J* 30 (3), pp. 215–221. DOI: 10.1295/polymj.30.215.

Fiedler, P.; Rätzsch, M.; Braun, D.; Michler, G. H. (1987): Einfluß des Knäueldurchmessers auf die Morphologie und die mechanischen Eigenschaften von Polyethylen. In *Acta Polym.* 38 (3), pp. 189–195. DOI: 10.1002/actp.1987.010380308.

Fillon, B.; Thierry, A.; Lotz, B.; Wittmann, J. C. (1994): Efficiency scale for polymer nucleating agents. In *Journal of Thermal Analysis* 42 (4), pp. 721–731. DOI: 10.1007/bf02546745.

Fischer, Simone (2021): Was die DIN SPEC 91446 für die Kreislaufwirtschaft bedeutet. In *plastverarbeiter*, 11/15/2021. Available online at <https://www.plastverarbeiter.de/preview-reader/din-spec-91446-veroeffentlicht->

822.html?postPreview=450166&postCheck=bf9c7a483f7975c373b75ab0c04e50c0, checked on 7/16/2023.957Z.

Florian J. Arbeiter; Andreas Frank; Gerald Pinter (2016): Influence of molecular structure and reinforcement on fatigue behavior of tough polypropylene materials. In *Journal of Applied Polymer Science* 133 (38). DOI: 10.1002/app.43948.

Freudenthaler, Paul J.; Fischer, Joerg; Liu, Yi; Lang, Reinhold W. (2022): Polypropylene Pipe Compounds with Varying Post-Consumer Packaging Recyclate Content. In *Polymers* 14 (23). DOI: 10.3390/polym14235232.

Frick, Achim (2011): *Praktische Kunststoffprüfung*. Edited by Claudia Stern. München: Hanser. Available online at <http://www.hanser-elibrary.com/doi/book/10.3139/9783446425750>.

Furukawa, Tsuyoshi; Sato, Harumi; Kita, Yasuo; Matsukawa, Kimihiro; Yamaguchi, Hiroshi; Ochiai, Shukichi et al. (2006): Molecular Structure, Crystallinity and Morphology of Polyethylene/Polypropylene Blends Studied by Raman Mapping, Scanning Electron Microscopy, Wide Angle X-Ray Diffraction, and Differential Scanning Calorimetry. In *Polym J* 38 (11), pp. 1127–1136. DOI: 10.1295/polymj.PJ2006056.

Geier, Jutta; Barretta, Chiara; Hinczica, Jessica; Bredács, Márton; Witschnigg, Andreas; Mayrbäurl, Erwin; Oreski, Gernot (2023a): Improving the quality of recycled polypropylene through sorting by processing method, unpublished. In *Waste Management*.

Geier, Jutta; Bredács, Márton; Witschnigg, Andreas; Vollprecht, Daniel; Oreski, Gernot (2023b): Analysis of different polypropylene waste bales – evaluation of the source material for PP recycling, submitted. In *Waste management & research*.

Grellmann, Wolfgang (2011): *Kunststoffprüfung*. 2. Auflage. München: Hanser Verlag. Available online at <http://www.hanser-elibrary.com/doi/book/10.3139/9783446429703>.

Grellmann, Wolfgang; Altstädt, Volker (2011): *Kunststoffprüfung*. 2. Aufl. München: Hanser. Available online at [http://sub-hh.ciando.com/book/?bok\\_id=270678](http://sub-hh.ciando.com/book/?bok_id=270678).

Guerrilla Agency (2022): What Is the Difference Between Polyethylene and Polypropylene? - MDI. Available online at <https://www.mdi.org/blog/post/what-is-the->

difference-between-polyethylene-and-polypropylene/, updated on 7/28/2022+00:00, checked on 4/3/2023.554Z.

Günzler, Helmut (2003): IR-Spektroskopie. Eine Einführung. 4., vollständig überarbeitete und aktualisierte Aufl (Online-Ausg.). Weinheim: Wiley-VCH GmbH & Co. KGaA. Available online at <http://site.ebrary.com/lib/alltitles/Doc?id=10565114>.

Hans-Josef Endres; Madina Shamsuyeva (2020): Warum die Kreislaufwirtschaft bessere Standards braucht. In *plastverarbeiter*, 7/2/2020. Available online at <https://www.plastverarbeiter.de/verarbeitungsverfahren/kunststoffrecycling/kreislaufwirtschaft-braucht-bessere-standards-857.html>, checked on 7/16/2023.994Z.

Hinczica, Jessica; Messiha, Mario; Koch, Thomas; Frank, Andreas; Pinter, Gerald (2022): Influence of Recyclates on Mechanical Properties and Lifetime Performance of Polypropylene Materials. In *Procedia Structural Integrity* 42, pp. 139–146. DOI: 10.1016/j.prostr.2022.12.017.

J. Schöne; I. Kotter; W. Grellmann (2012): Properties of Polypropylene Talc Compounds with different talc particle size and loading. In *Zeitschrift Kunststofftechnik/ Journal of Plastics Technology* (2), pp. 230–251. Available online at [https://www.researchgate.net/publication/286521731\\_Properties\\_of\\_Polypropylene\\_Talc\\_Compounds\\_with\\_different\\_talc\\_particle\\_size\\_and\\_loading](https://www.researchgate.net/publication/286521731_Properties_of_Polypropylene_Talc_Compounds_with_different_talc_particle_size_and_loading).

DIN EN ISO 11357-1: Kunststoffe\_ - Dynamische Differenz-Thermoanalyse\_(DSC)\_ - Teil\_1: Allgemeine Grundlagen (ISO\_11357-1:2016); Deutsche Fassung EN\_ISO\_11357-1:2016.

ONR CEN/TS 14541-2, 5/1/2023: Kunststoff-Rohrleitungen und -Formstücke - Verwendung von thermoplastischen Rezyklaten.

Kunststoffrohrverband e.V. - Fachverband der Kunststoffrohr-Industrie (2022): Rohr-Recycling. Available online at <https://www.krv.de/wissen/rohr-recycling>, updated on 10/27/2022, checked on 10/27/2022.

Kunststoffrohrverband e.V. - Fachverband der Kunststoffrohr-Industrie (2023): Rohr-Recycling. Available online at <https://www.krv.de/wissen/rohr-recycling>, updated on 7/4/2023, checked on 7/4/2023.

Lapcik, Lubomir; Jindrova, Pavlina; Lapcikova, Barbora (2009): Effect of Talc Filler Content on Poly(Propylene) Composite Mechanical Properties. In : Engineering Against Fracture: Springer, Dordrecht, pp. 73–80. Available online at [https://link.springer.com/chapter/10.1007/978-1-4020-9402-6\\_6](https://link.springer.com/chapter/10.1007/978-1-4020-9402-6_6).

Lustiger, Arnold (1986): Environmental Stress Cracking. The Phenomenon and its Utility. In Witold Brostow, Roger D. Corneliussen (Eds.): Failure of plastics. Munich, New York: Hanser; Hanser Pub.; Distributed in the United States of America by Macmillan Pub., pp. 305–329.

Lustiger, Arnold; Ishikawa, N. (1991): An Analytical Technique for Measuring Relative Tie-Molecule Concentration in Polyethylene. In *J Polym Sci Polym Phys* (29), pp. 1047–1055. DOI: 10.1002/polb.1991.090290902.

Maier, Clive; Calafut, Teresa (1998): 4 - Fillers and reinforcements. In Clive Maier, Teresa Calafut (Eds.): Polypropylene. The definitive user's guide and databook. Norwich, NY: Plastics Design Library (PDL handbook series), pp. 49–56. Available online at <https://www.sciencedirect.com/science/article/pii/B9781884207587500096>.

Maiti, S. N.; Sharma, K. K. (1992): Studies on polypropylene composites filled with talc particles. In *Journal of Materials Science* 27 (17), pp. 4605–4613. DOI: 10.1007/bf01165994.

Mallick, P. K. (2006): 2.09 - Particulate and Short Fiber Reinforced Polymer Composites. In Anthony Kelly, Carl Zweben (Eds.): Comprehensive composite materials. Amsterdam: Elsevier, pp. 291–331. Available online at <https://www.sciencedirect.com/science/article/pii/B0080429939000851>.

Martín-Martínez; José Miguel (2002): Chapter 13 - Rubber base adhesives. In Manoj Kumar Chaudhury (Ed.): Adhesion Science and Engineering. Surfaces, Chemistry and Applications. With assistance of A. V. Pocius, D. A. Dillard. Amsterdam: Elsevier Science & Technology (Adhesion Science and Engineering, v.1 & 2), pp. 573–675. Available online at <https://www.sciencedirect.com/science/article/pii/B9780444511409500135>.

McLauchlin, A. R.; Thomas, N. L. (2009): Preparation and thermal characterisation of poly(lactic acid) nanocomposites prepared from organoclays based on an amphoteric

surfactant. In *Polymer Degradation and Stability* 94 (5), pp. 868–872. DOI: 10.1016/j.polymdegradstab.2009.01.012.

Messiha, Mario; Frank, Andreas; Koch, Thomas; Arbeiter, Florian; Pinter, Gerald (2020): Effect of polyethylene and polypropylene cross-contamination on slow crack growth resistance. In *International Journal of Polymer Analysis and Characterization* 25 (8), pp. 649–666. DOI: 10.1080/1023666X.2020.1833143.

Mettler-Toledo (2022): PVC Measured by DSC and TGA. Mettler-Toledo International Inc. all rights reserved. Available online at [https://www.mt.com/at/de/home/supportive\\_content/matchar\\_apps/MatChar\\_HB220.html](https://www.mt.com/at/de/home/supportive_content/matchar_apps/MatChar_HB220.html), updated on 7/19/2023.000Z, checked on 7/19/2023.537Z.

Mettler-Toledo Inc. all rights reserved (2022): Dynamisch-mechanische Analyse (DMA). Mettler-Toledo International Inc. all rights reserved. Available online at [https://www.mt.com/at/de/home/products/Laboratory\\_Analytics\\_Browse/TA\\_Family\\_Browse/DMA.html](https://www.mt.com/at/de/home/products/Laboratory_Analytics_Browse/TA_Family_Browse/DMA.html), updated on 10/12/2022.000Z, checked on 10/12/2022.157Z.

Pinter, Gerald (1999): Rißwachstumsverhalten von PE-HD unter statischer Belastung.

ISO 527, 2012: Plastics -- Determination of tensile properties.

ISO 1133, 2005: Plastics -- Determination of the melt mass-flow rate (MFR) and the melt volume-flow rate (MVR) of thermoplastics.

ISO 11357, 2002: Plastics -- Differential scanning calorimetry (DSC).

PlasticsEurope (2020): Plastics - the Facts 2020. An analysis of European plastics production, demand and waste data. Brussels.

PlasticsEurope (2022): Plastics - the Facts 2022. Brussels.

ISO 18489, 2015: Polyethylene (PE) materials for piping systems -- Determination of resistance to slow crack growth under cyclic loading -- Cracked Round Bar test method.

ISO 18489: Polyethylene (PE) materials for piping systems — Determination of resistance to slow crack growth under cyclic loading — Cracked Round Bar test method.

DIN EN ISO 9001, 2015: Qualitätsmanagementsysteme\_ - Anforderungen (ISO\_9001:2015); Deutsche und Englische Fassung EN\_ISO\_9001:2015. Available online at <http://dx.doi.org/10.31030/2325651>.

Ragaert, Kim; Delva, Laurens; van Geem, Kevin (2017): Mechanical and chemical recycling of solid plastic waste. In *Waste management (New York, N.Y.)* 69, pp. 24–58. DOI: 10.1016/j.wasman.2017.07.044.

Recycled PP - cirplus (2023). Available online at <https://www.cirplus.com/materials/recycled-pp>, updated on 6/7/2023, checked on 6/7/2023.

Sinha Ray, Suprakas; Yamada, Kazunobu; Okamoto, Masami; Ueda, Kazue (2002): Polylactide-Layered Silicate Nanocomposite: A Novel Biodegradable Material. In *Nano Letters* 2 (10), pp. 1093–1096. DOI: 10.1021/nl0202152.

Stafford, Trevor. (2001): The European plastic pipes market. a Rapra industry analysis report /. Shawbury, Shrewsbury, Shropshire, UK: Rapra Technology Ltd.,

Statista (2023): Statista - The Statistics Portal. Available online at [https://www.bcp.fu-berlin.de/chemie/chemie/studium/ocpraktikum/\\_Unterlagen\\_Spektroskopie/ir.pdf](https://www.bcp.fu-berlin.de/chemie/chemie/studium/ocpraktikum/_Unterlagen_Spektroskopie/ir.pdf), updated on 4/4/2023, checked on 4/4/2023.

Steinko, Willi (2008): Optimierung von Spritzgießprozessen. München: Hanser.

Strömberg, Emma; Karlsson, Sigbritt (2009): The design of a test protocol to model the degradation of polyolefins during recycling and service life. In *Journal of Applied Polymer Science* 112 (3), pp. 1835–1844. DOI: 10.1002/app.29724.

Tripathi, Devesh (2002): Practical Guide to Polypropylene: iSmithers Rapra Publishing.

University of Tartu (2023a): Talc – Database of ATR-FT-IR spectra of various materials. Edited by WordPress. Institute of Chemistry University of Tartu, Department of Geology, Estonia. Available online at <https://spectra.chem.ut.ee/paint/fillers/talc/>, updated on 2023-07, checked on 7/20/2023.311Z.

University of Tartu (2023b): Chalk – Database of ATR-FT-IR spectra of various materials. Edited by WordPress. Institute of Chemistry University of Tartu, Department of Geology,



Estonia. Available online at <https://spectra.chem.ut.ee/paint/fillers/chalk/>, updated on 2023-07, checked on 7/20/2023.381Z.

Utracki, Leszek A.; Wilkie, Charles A. (Eds.) (2014): Polymer blends handbook. 2. ed. Dordrecht: Springer (Springer reference, 3).

Villanueva Krzyzaniak, Alejandro; Eder, Peter (2014): End-of-waste criteria for waste plastic for conversion. Technical proposals. Edited by Publications Office of the European Union.

W.C.J Zuiderduin; C Westzaan; J Huétink; R.J. Gaymans (2003): Toughening of polypropylene with calcium carbonate particles. In *Polymer* 44 (1), pp. 261–275. DOI: 10.1016/S0032-3861(02)00769-3.

Yanwei Jing; Xueying Nai; Li Dang; Donghai Zhu; Yabin Wang; Yaping Dong; Wu Li (2018): Reinforcing polypropylene with calcium carbonate of different morphologies and polymorphs. In *Science and Engineering of Composite Materials* 25 (4), pp. 745–751. DOI: 10.1515/secm-2015-0307.

